Patient specific Long QT syndrome type 3 cardiomyocytes can be used for clinical drug safety assessments Masterproef ingediend met het oog op het behalen van de graad van Master in…

Thesis · May 2018

CITATIONS
0

READS
32

2 authors, including:

Ben Bohlen
Vrije Universiteit Brussel
2 PUBLICATIONS **0** CITATIONS

SEE PROFILE

VRIJE UNIVERSITEIT BRUSSEL

Masterproef ingediend met het oog op het behalen
van de graad van Master in de Geneeskunde

2017-2018

Promotor: Prof. Dr. Pedro Brugada

Scientific Director, Cardiovascular Division
Free University of Brussels (UZ Brussel) VUB

Laboratory: Axiogenesis, Cologne Germany

Geneeskunde en Farmacie

Patient specific Long QT syndrome type 3 cardiomyocytes can be used for clinical drug safety assessments

B. Bohlen and P. Brugada

Abstract

Long QT syndrome is a heart rhythm disorder with a prolonged QT interval which can result in a torsade de pointes tachycardia and ventricular fibrillation leading to sudden cardiac death. To date, there are 14 subtypes known with multiple different genes and locations of the mutation causing the disease that is either inherited or caused by de-novo mutations. In addition, a prolonged QT interval can be acquired due to adverse drug effects mostly blocking the outward rectifying potassium channel (hERG).

Cardiomyocytes (CM) were generated from a Long QT syndrome type 3 (LQT.3) patient using the same SMAD-activated differentiation approach as for a healthy control cell line (CorV.4U). LQT.3 CMs were subjected to electrophysiological analysis using patch-clamp-, multi electrode array- (MEA), calcium cycling-, impedance- and contractile force-measurements. Pharmacological analysis was done with model substances to evaluate the drug effects and arrhythmogenic potential. For the comparative analysis CorV.4U were used as a healthy control cell line. Furthermore, LQT.3 CMs were electrically paced to induce arrhythmias.

The MEA experiments demonstrate a higher sensitivity in measuring prolongation of field potential duration using the LQT.3 CMs model as compared to other CM models in pharmacological studies. Field potential prolongation and QT prolongation can be directly linked and are thus associated with a higher risk in arrhythmic events. This enables this CM model to be used in pharmacological safety testings to detect cardiac adverse drug effects in early pre-clinical phases. Moreover, LQT.3 CMs can be used to study the pathophysiology of the Long QT syndrome.

Table of content

1. Introduction and background

Long QT syndrome (LQTS) is a rhythm disorder characterized by a prolonged heart-rate corrected QT interval (QTc ≥ 450 ms for men, ≥ 460 ms for women) [1]. Patients typically have slow heart rates and suffer from cardiac like syncopes caused by a variety of mechanisms, among them polymorphic ventricular tachycardia (known as torsade de pointes, TdP) and sudden cardiac death (SCD), mostly due to ventricular fibrillation [2,3,4,5]. LQTS is a hereditary disorder with 80 % of the cases caused by inherited and 20 % a de-novo mutation. LQTS is inherited as an autosomal dominant disorder known as the Romano-Ward Syndrome (LQTS 1 - 14, 70%) [6,7] or as an autosomal recessive disease known as the Jervel-Nielsen-Lange-Syndrome (JNL 1 - 2, 30 %) [8,9] with distinct characteristics on the electrocardiogram (ECG). Beside the mutations also single nucleotide polymorphisms (SNPs) in non-coding regions are known as 'QT-interval modifier' [4,9,10]. The majority of these mutations result in asymptomatic chanellopathies with a delayed onset of symptoms or can cause acute severe heart rhythm disorders [11]. The dangerous aspect of this spectrum of heart rhythm disorders is the silent onset of symptoms, except for the JNL syndrome that is associated with congenital deafness [12]. The spectrum of clinical presentation is broad, from fully asymptomatic individuals to SCD. SCD can occur without any preceding symptoms or with syncopes being the only warning symptom before SCD.

There are 16 variations of the LQTS which can be caused by alterations in more than 20 genes, each known with several hundred different mutations [6,10,13]. LQT.1 - LQT.3 are the most prevalent types of LQTS. Loss of function mutations in the potassium channel genes KCNQ1 (LQT.1) and KCNH2 (LQT. 2) lead to a reduced repolarization in phase 3 of the action potential (AP) by affecting the rapid delayed rectifier current (I_{Kr}). Mutations in the SCN5A gene causing the LQT.3 syndrome phenotype lead to a gain-of-function in the fast acting sodium channel ($Na_V1.5$), enhancing the fast sodium current (I_{Na}). In phase 1 of the action potential (AP) the ion channel is not fully inactivated leading to a prolonged action potential generation. Even more, the late sodium current ($I_{Na,L}$) in phase 2 is prolonged which gives rise to a prolongation of the depolarization in phase 2 and 3 of the AP and leads to a delayed repolarization (see figure 1 for the cardiac AP phases). This results in an increased risk for early afterdepolarization (EAD) and delayed afterdepolarization (DAD) by a recovery from inactivated calcium transients in phase 2 and 3 of the AP [14]. EADs can be triggers for ventricular tachycardias (TdP), ventricular fibrillation and arrhythmic heart rhythms as paroxysmal atrial fibrillation [9]. LQTS type 3 appears to be the most malignant. The phenotype of electrophysiological alterations depends on the localization of the mutation. This implicates that de-novo mutations in important ion channels can either be silent and have no influence on ion current kinetics or moderate to highly symptomatic if the mutation is located in regulatory or permeability defining domains [15].

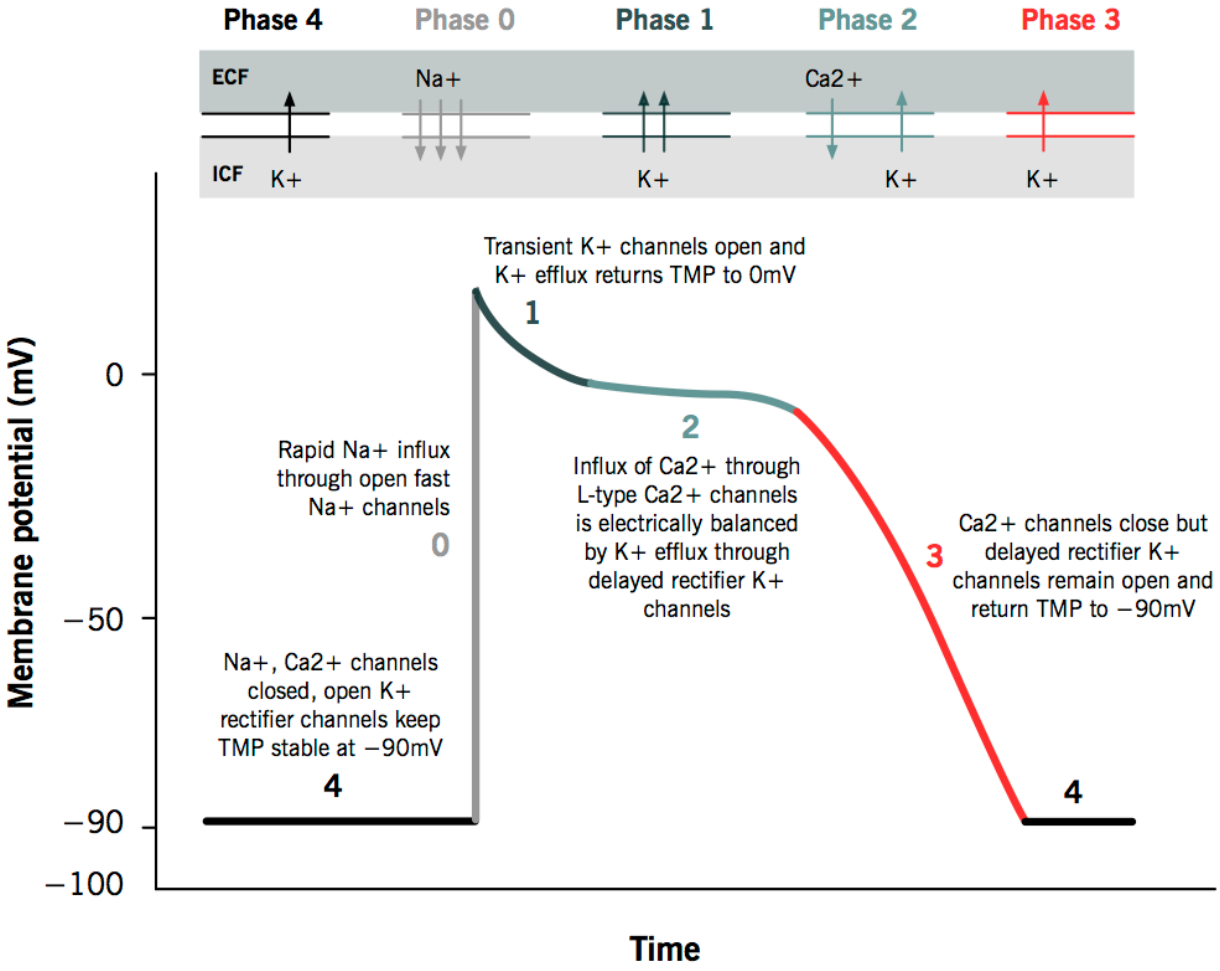

Figure 1 Cardiac action potential and the sequence of well concerted ion channel activities are shown. Phase 0 represents the fast opening of voltage gated sodium channels and influx of sodium ions. TMP (transmembrane potential) is raised by 90 - 100 mV from a mean resting potential of - 90 mV to 10 mV. In Phase 1, a small amount of potassium channels is opened and TMP is brought to ± 0 mV. Voltage-gated calcium channels are opened in phase 2 of the action potential leading to a calcium-induced calcium release. This enables cardiomyocytes for contraction. Phase 3 resembles the depolarization of CMs by opening delayed rectifying potassium channels bringing the cell to a resting TMP of - 90 mV [16].

Apart from patients with congenital LQTS there is also an iatrogenic cause for a clinically relevant LQTS. Patients without cardiac pathologies can develop QT prolongation due to adverse drug reaction (ADR) or due to serum ion concentration disorders. The QT prolongation is an adverse effect mostly resulting from the inhibition of the outward rectifying potassium current $K_V11.1$ (I_{Kr}) in phase 3 of the AP. Medications that can cause QT prolongation are antibiotics like moxifloxacin, gatifloxacin [17] and erythromycin, anti-arrhthymic drugs sotalol and chinidine, anti-psychotic drugs (eg. chlorpromazine) and many others [18]. Overdoses as well as enzyme inhibition or slow-metabolizers leading to accumulation of QT prolonging drugs can also result in this pathological effect. Recently a drug-drug interaction was described that can also be associated with a QT-prolongation whereas these drugs alone did not cause any changes in the QT-interval [19]. Metoprolol and fosphenytoin as well as cefazoline and lansoprazole cause a significant increase in the QTc-interval when used in combination [19].

QT prolongation and the possible resulting life threatening arrhythmias (TdP, VT, absolute bradyarrhythmia) are indications for withdrawal of existing medications as for example grepifloxacin and cisapride from the market [17,18]. Furthermore, QT prolongation in drug candidates is an indication for abandoning these drug candidates from clinical studies. Currently, these analysis are sub-summarized under the form of hERG liability testing in phase I drug testings whereby the majority of assay systems consist of relatively unphysiological cell systems with transgenic lines (xenopus oocytes, human kidney cells, Chinese hamster ovary) [20] in which certain ion channels are over-expressed, thus neglecting up- and downstream events of the analyzed (e.g. hERG) channel and drug effects on the ion homeostasis in beating cardiomyocytes (CMs). Sodium channel expression patterns seem also to be different in these systems as compared to CMs. In a recent study, initiated by the FDA within the Comprehensive in-vitro Proarrhthymia Assay (CiPA) study group, human induced pluripotent stem cells (hiPSC) derived CMs are analyzed as a replacement for the latter mentioned artificial cell system [21,22]. HiPSC derived CMs are a relevant alternative to test the cardiac side effects of drugs as they express all relevant ion channels as well as regulatory elements. Therefore these models are evaluated in the prediction of adverse cardiac effects. Until now, there are just a few standardized cardiomyocyte cell lines (iCell - CDI, Cor.4U - Axiogenesis) available [23]. Recently described disease models for inherited heart rhythm disorders are still experimental [24]. Proper functional research has been limited by the absence of standardized differentiation attempts and suitable techniques for an objective evaluation [23]. Furthermore, there is a wide inter-laboratory disconcordance regarding differentiation protocols, execution of tests and the data analysis [23,24,25].

Mutation associated arrhythmias are best studied in CM cultures in in-vitro experiments. After reviewing the risk and limitations of taking cardiac biopsies from affected patients for study purposes, patient derived iPSCs offer a new possibility for the development of treatment strategies and research on the pathophysiological mechanisms of genetic inherited syndromes [10]. Nearly every individual mutation associated disease can be studied in-vitro using the hiPSC technologies. These cells can be cultured to an unlimited amount of pluripotent cells for the differentiation of for example cardiac tissue and can be generated from any tissue that is available. HiPSCs have great advantage compared to other cell sources such as murine embryonic stem cells (mESC), human embryonic stem cells (hESC), transgenic cell lines and animal models. There are significant differences between murine and human physiology. The heart of a mouse beats approximately ten times faster than the human hart. Furthermore the hERG channel is not used for repolarization as in human CMs implicating that hiPSC are much more physiological compared to murine ESC. HESC reflect human physiology and complexity of ion homeostasis but are difficult to cultivate and difficult to obtain due to ethical concerns. With the use of hiPSC in pharmacological safety testings, ethical considerations concerning the origin of hESC can be overcome.

The purpose of this study is to show that a standardized protocol can be used for the differentiation and generation of spontaneous beating LQT.3 CMs. Furthermore it is essential to describe the phenotype of LQT.3 CMs and its' electrophysiological characteristics. It is hypothesized that the electrophysiological phenotype of LQT.3 CMs will be different to the phenotype of healthy control CMs.

The study describes how hiPSCs derived LQT.3 CMs responded to drugs used in daily clinically routine in comparison to healthy hiPSC. Hereby we postulate an increased sensitivity for the QTc-prolonging effects of several cardiac and non-cardiac drugs listed in table 1 on LQT.3 CMs compared to healthy hiPSC derived CMs, as for example Cor.4U CMs. The latter are standardized hiPSC derived CMs with a healthy phenotype (including defined donor with a full medical check-up and family analysis). Another aim of this study is to document the induction of arrhythmias in electrophysiological studies of LQT.3 CMs as a proof of concept for physiological-like experiments. Drug induced loss of repolarization ability as well as brady- and tachyarrhythmia and asystolie (beating arrest) are endpoints in the electrophysiological characterization of LQT.3 CMs.

Multi-electrode array (MEA) measurement is a technique that visualizes extracellular field potentials (FP) of in-vitro differentiated CMs but also neurons and other cells [21]. MEA measurements are performed by recording multiple channels from an array of incorporated electrodes in a cell culture plate. The recorded FPs represent the configuration and time course of the action potential in hiPSC derived CMs [21]. FPs from CMs reflect the AP (phase 0 - 4) and the QT-interval on an ECG in clinical practice. A prolongation of the FP duration (FPD) in-vitro correlates with a QT-prolongation in vivo. In contrast to the patch clamp technique, MEA recording can be performed in a medium to high throughput setting and does not require a modified environment, thus mirroring a physiological situation. **This implicates that the former golden standard of patch-clamping can be replaced with the measurement of FPs by MEA**, thus improving and strengthening the idea of a physiological cell system for clinical testing. Patch clamp analysis will be performed to verify the collected data from MEA measurements. Patch clamp is a technique that facilitates the measurement of transmembrane voltage and specific currents flowing across the membranes. Glass micropipettes that are connected to a micro electrode „puller" rupture the membrane in the opening of the pipette. Consequently, a tight electrical junction between lipid bilayers and the glass is created. The tip of each pipette is filled with an internal solution that is selected for the analyzed cell. The solution will form an electrical seal to prevent ion exchange from the cell to solution. The use of the patch clamp technique is thereby a significant modification in the ion homeostasis of beating CMs.

Moreover, a prolonged depolarization due to a prolonged activation of sodium channels causes a premature re-opening of voltage gated calcium channels. Thereby, not only FP should be analyzed regarding the influence of drugs on cardiac repolarization but also intracellular calcium transients. Recent studies indicate the influence of calcium-dependent mechanisms on the generation and formation of EADs [26] leading to malignant rhythm disorders. By measuring calcium, calcium dependent EAD formation can be documented and studied.

2. Material and methods

2.1. Preparation of LQT.3 hiPSC

The donor for cell material was a 19 year old Caucasian Hispanic woman affected with the LQTS and a Bazett's corrected QT-prolongation of 523 ms and T-wave abnormalities on the 12-lead ECG. The disease was caused by a de-novo mutation (there was no clinical history of other diseases or LQTS identified in the family). Due to privacy reasons there is no other information known about the clinical history of the donor patient [27].

Human induced pluripotent stem cells (hiPSC) were created from a skin punch biopsy of dermal fibroblasts and reprogrammed with retroviruses by Coriell (USA) after expansion of primary fibroblasts. Long QT syndrome type 3 (LQT.3) hiPSCs were cultured on Matrigel® (Corning) in mTeSR™ feeder-free cell culture medium (Stemcell Technologies) with 20% Knock-out Serum Replacement and expanded. Cells were frozen at passage 25 at Coriell and offered for scientific research [27].

Patient specific LQT.3 hiPSCs were obtained from Coriell and passaged three times before transfection with a vector containing a puromycin resistance gene for purification of cardiac cells after differentiation. A neomycin resistance cassette driven by the cytomegalovirus promotor was also cloned into the vector to facilitate a selection of successfully transfected LQT.3 iPSCs. For cardiac differentiation the well known cardiac-specific alpha-MHC promotor was chosen for the expression of the puromycin resistance gene. This promotor is expressed in atrial and ventricular tissue. An internal ribosome entry site (IRES) was used downstream of the puromycin resistance gene to promote a high expression rate and to ensure translation of the puromycin resistance gene product.

Briefly, $1x10^6$ LQT.3 iPSC's were transfected by improved electroporation with 5μg vector using the Nucelofactor™ Technology (Lonza). Transfected hiPSCs were seeded on Matrigel coated culture dish (50 μL/cm^2) and cultured in StemMACS™ iPS medium with StemMac Supplement (Miltenyi Biotech, Germany). 24 hours after transfection, neomycin (400 μg/mL, LifeTechnologies, NJ) was added to select successfully transfected hiPS cells. Three days after transfection, several colonies grew under selection conditions. When cells grew out to sharp lined colonies of approximately 1 mm^2, colonies were picked after a incubation of 5 minutes in citrate buffer and further expanded in culture flasks (Nunc™ T75/175, ThermoFischer Scientific) using the same coating and StemMAC iPS medium with supplement. Cells were passaged twice before harvesting and three further passages were performed before freezing cells as a master stock for large-scale differentiation.

Randomly selected clones of LQT.3 hiPSC were passaged and seeded in T25 culture flask coated with Matrigel® in StemMACS iPS medium with StemMac Supplement. The cells were cultured for three days and dissociated, when colonies were confluently grown, using calcium citrate and replated in T175 culture flasks at a split rate of $5x10^6$ cells/T175 flask. ROCK Inhibitor (2 μM, Y-27632 dihydrochloride, Tocris) was added after dissociation. LQT.3 hiPSC were expanded three times to generate enough hiPSC for differentiation.

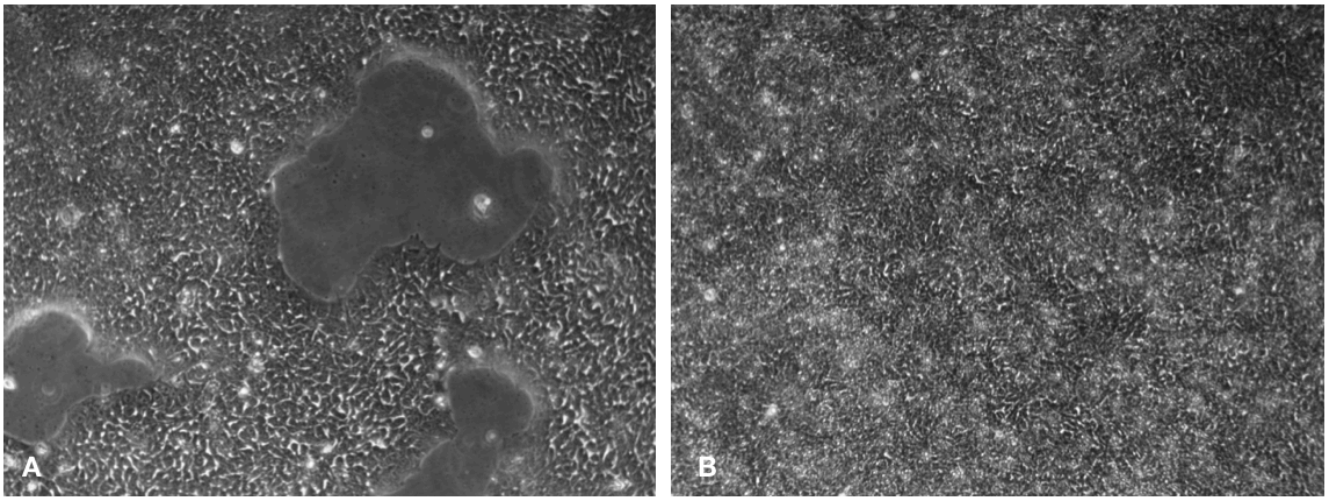

Figure 2 - HiPSC morphology. Panel A shows hiPSC two days after dissociation. Note the well shaped colonies border and the confluent growth of the cells which is reached after 3 days as shown in panel B.

2.2. Differentiation of LQT.3 cardiomyocytes

At passage four, LQT.3-hiPSC were dissociated with calcium citrate and plated in 6-Well culture plates coated with fibronectin (1 μg/mL in phosphate buffered saline - PBS - with Ca/Mg, Sigma Aldrich) at a density of 1,25 x 10^5 cells per cm^2 in Gibco® RPMI medium 1640 (Pan) with 1 mg/mL human serum albumin (HSA, Sigma-Aldrich), 2 mg/mL Ciprofloxacin (Bayer) and 220 μg/mL ascorbic-acid-2-phosphate (Sigma Aldrich). ROCK Inhibitor (2 μM, Y-27632 dihydrochloride, Tocris, Catalog No. 1254) was added on the first day of differentiation [33,34]. On the next day 15 μM of the GSK3β inhibitor Chir990021 (Tocris, Catalog No 4423) was added and cells were incubated for exact 24 hours [34,35]. Chir990021 was titrated from doses of 6 μM to 15 μM in order to find the most efficient concentration for a cardiac differentiation. Chir990021 was washed out and replaced by RPMI medium 1640 (Pan) containing 1 mg/mL HSA (Human serum albumin, Tocris) [35,37]. 48 hours after initiation of differentiation, canonic WNT-inhibition was induced for mesodermal differentiation for further 48 hours by adding 9-12 μM XAV939 (Tocris, Catalog No. 3748), 8 μM WNT-c59 (Tocris, Catalog No 5148), and 1 μM Retinoid Acid (Sigma Aldrich, CAS number 302-79-4) [41]. After 2 days of incubation with the WNT-inhibiting molecules, the differentiation medium was washed out and replaced with defined RPMI medium with 1 mg/mL HSA. 75 ng/mL Human IGF-1 (Sigma Aldrich) was added on day 6 [36]. Cells showed characteristic growth pattern under different concentrations of the compounds mentioned above. On day 8, cells showed spontaneous beating activity. RPMI 1640 medium was replaced by IMDM medium (Iscove's Modified Dulbecco's Medium, PAN) on day 10. After 11 days the vast majority of the well showed spontaneous beating activity. CMs were selected using puromycin (1μg/mL). Pure CMs were obtained 5-10 days after selection. Cells were harvested and pooled by digestion with 0,1 % Trypsin for further culturing, maturation and testing. See figure 3 for a brief overview.

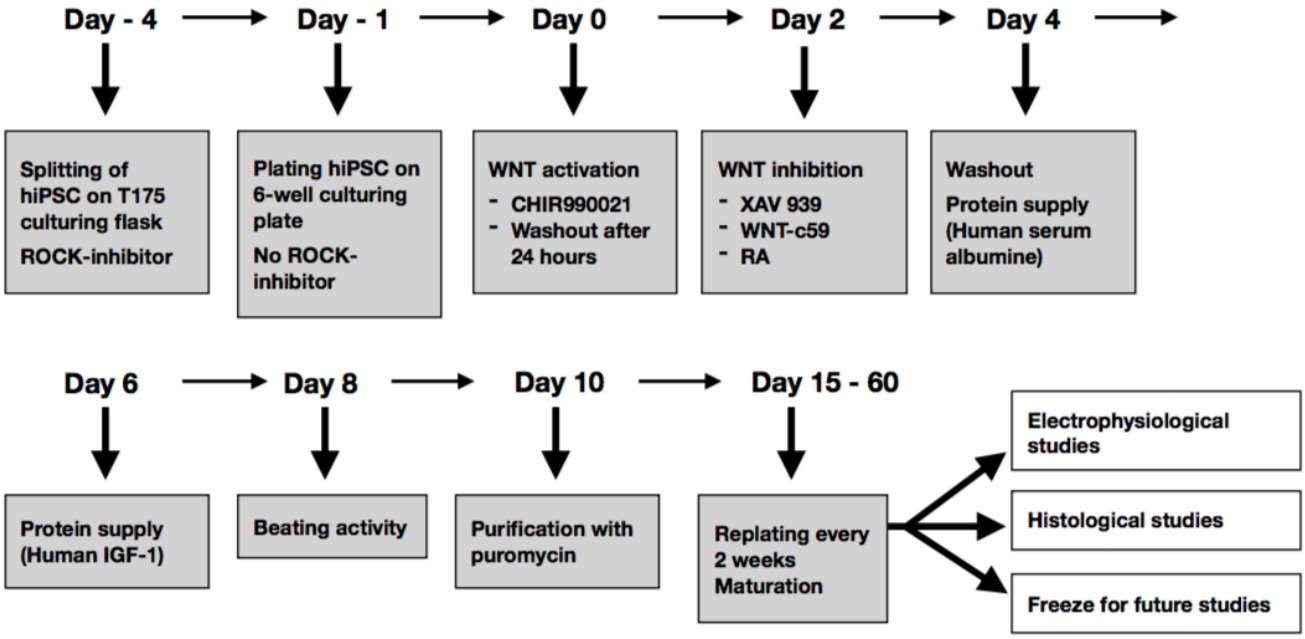

Figure 3 Chronology of molecular steps that are needed in a successful cardiac differentiation approach. WNT activation is initiated by CHIR. After two days, WNT inhibition is performed using XAV, WNT-c59 and RA. After two days of incubation the WNT modulation is completed and small molecules are washed out. Cells are treated with an increased amount of protein. On day 8, spontaneously beating was observed. CMs were purified with puromycin (1 ng/mL) and then cultured for several weeks to let CMs mature.

2.3. Culturing of LQT.3 cardiomyocytes

Pure LQT.3 CMs were cultured for 6 - 8 weeks on fibronectin coated T175 culture flask, at a density of 1,5 x 10^5 cells per cm^2. The CMs were cultured in CM culturing medium containing IMDM with 5 % fetal calf serum (FCS, Pan), 215 mg/mL Ciprofloxacin (Bayer), 220 μg/mL ascorbic-acid-2-phosphate (Sigma Aldrich) and 12,5 μg/mL insulin (Sigma-Aldrich). Medium was changed every three days. Sterility controls were examined before each interaction with the cells.

LQT.3 CMs were dissociated following the protocol mentioned earlier and seeded in the specific testing plates (figure 3). Compound tests were performed in CM culturing medium with vehicle concentrations < 0,001 % DMSO or PBS w/o Ca/Mg.

Cryopreserved standardized hiPSC derived ventricular and atrial CMs (CorV.4U and CorA.4U, Axiogenesis) were obtained and slightly thawn in pre-warmed medium followed by culturing in Cor.4U medium according to the manufacturing protocol. One week after culturing of CMs, cells were dissociated from the monolayer culture plate by incubating the cells in 0,1 % Trypsin for five minutes. Single cell suspension was created by suspending the cells for up to five times. The cells were counted and replated on fibronectin coated culture flasks or intervention culture formats (96-well MEA plate, Corning® 96 μcell plates with clear bottom for Ca^{2+} assay, Nanion Sensor Plate® (NSP) 96-well culture plates for base impedance, 48-well plate for immunostaining, 8-well drum plate for contractile force measurement).

2.4. Immunofluorescence analysis of LQT.3 cardiomyocytes

Matured LQT.3 CMs were plated at density of 5 x 10^4 and 10^5 cells/well in a fibronectin coated 48 well culture plate and cultured for three days in CM culturing medium. CMs were washed with PBS with Ca/Mg twice and fixated using 4 % paraformaldehyde in PBS w/o Ca/Mg with a pH of 7,4 for 60 minutes at room temperature (RT). After fixation cells were washed three times with ice-cold PBS w/o Ca/Mg for 10 minutes. Cells were permeabilized with 0,1 % Triton-X-100 (Sigma Aldrich) and aspecific protein binding was blocked with 10 % Native Goat Serum (NGS, Sigma Aldrich). For the prevention of uncontrolled membrane destruction, cells were washed three times with PBS w/o Ca/Mg for 10 minutes. The primary antibodies (ABs) were added for intracellular target binding.

LQT.3 CMs were stained with the following antibody combination: anti-MCL-2V (anti-rabbit IgG, pAb, 1,2 mg/ml, 1:500 dilution, Thermo Fischer) and anti-Troponin (anti-mouse IgG, pAb, 0,2 mg/mL, 1:200 dilution, Thermo Fischer), anti-MLC-2A (anti-mouse IgG, pAb, 1 mg/mL, 1:200 dilution, Thermo Fischer) with anti-Connexin40 (anti-rabbit IgG, pAb, 0,25 mg/mL 1:200 dilution, Thermo Fischer), anti-Connexin43 (anti-rabbit IgG, pAb, 0,25 mg/mL, 1:500 dilution, Thermo Fischer) and anti-alpha-Actinin (anti-mouse IgG, mAb, 1 mg/mL, 1:200 dilution, Thermo Fischer). Primary ABs were diluted in PBS w/o Ca/Mg with 0,1 % Triton-X-100 (Thermo Fischer) and 1% NGS (Thermo Fischer) and incubated over night at 4°C. The solution was decanted and secondary ABs (Alexa-Fluor468 anti-mouse IgG and Alexa-Fluor555 anti-rabbit IgG, pAb, 2 mg/ml, 1:200 dilution, Thermofischer) were added in PBS with 1 % NGS. Secondary ABs were incubated at RT in the dark for one hour. After decanting the secondary AB, cells were washed three times with PBS w/o Ca/Mg for 10 minutes in the dark at RT. DAPI (1 µg/mL, dilution 1:10^4, Thermo Fischer) was added at the last step of the wash-out and incubated for 10 minutes. After the wash-out of DAPI, cells were ready for analysis.

Immunofluorescent analysis was performed with a Zeiss Axioplan microscope, containing a Cy3, FITC and Hoechst filter to detect the secondary ABs. VisiView 2.1 (Visitron Systems, Germany) was used to generate high quality images and overlay pictures.

2.5. Transfection of LQT.3 CMs and CorV.4U CMs cells with ChR2-mRNA

LQT.3 and CorV.4U CMs were transfected with stable capped mRNA (messenger ribonucleotide acid) (Express.4U) encoding a sodium channel that is reactive to light stimulation with a wavelength of 460 nm, Channel Rhodopsin 2 (ChR2) [28]. 1,5 ng/μL ChR2 mRNA was used for the transfection of one 96 well plate following the Express.4U (Axiogenesis, Germany) instructions and incubated for another day. The next day cells were used for analysis. LQT.3 and CorV.4U CMs were tested with the mRNA encoded ChR2 on the MEA system using a optical stimulation unit (Nanion Systems) [28].

2.6. Electrophysiological characterization of LQT.3 CMs

2.6.1. MEA analysis

The region of each electrode field on the 96-well MEA plates (Axion Biosystems) was incubated with 6 μL Geltrex® (Thermo Fischer) at 37°C for 30 minutes in a humid chamber. CMs were dissociated from long-term cultures to obtain single cell suspension using a 0,1 % trypsin digestion for 5 minutes (figure 3). After incubation, geltrex was aspirated and 10^5 CMs were seeded in a drop of 5 μL on the central

electrode of the well in order to avoid touching the bottom with the pipette tip. The plate was incubated for three hours at 37°C in a humid chamber to facilitate cell adhesion on the electrodes. After incubation each well was filled up with 200 μL CM culturing medium and medium was changed every two days.

Medium was changed at the day of FP measurements. Before recording field potentials, CMs were equilibrated for 60 minutes at 37°C and 5 % CO_2.

FPs were detected using the Axion MEA System (Nanion, Germany) with a highpass filter of 0,1 - 2,5 Hz, as Sawada et al recommend this filter setting in dose dependent studies, and digitalized with AXis® (Axion integration system, Axion, Germany) and the CiPA analysis tool. The CiPA tool generated an average beat over 120 seconds recording time with a cut-off value for FP amplitude ≥ 100 μV for LQT.3 CMs and ≥ 300 μV for CorV.4U and Cor.A4U for the first positive deflection and ≥ 15 μV for the second deflection (positive or negative) [23] as shown in figure 4 A. Minimum beat frequency was five beats per minute. EAD, DAD, triggered activities (TA) and tachyarrhythmia were digitalized with CiPA plotting tool (Axion) and plotted as single beat. FPD was corrected using the Bazetts QT correction formula (FPDcB) for beat rates between 60 and 100 beats per minute (bpm) and Fridericia QT correction formula (FPDcF) for beat rates above 100 bpm. Temperature was monitored during measurements and kept at 37°C for a stable ion channel function and to prevent temperature-dependent dysregulation of hERG channels [29]. Several arhythmic events can be detected using MEA recordings as shown in figure 4 B. Mean analysis of the LQT.3 phenotype was analyzed with n = 80. Drug effects were tested with n = 3 per concentration. Mean FPD and frequency calculated and corrected with the standard deviation.

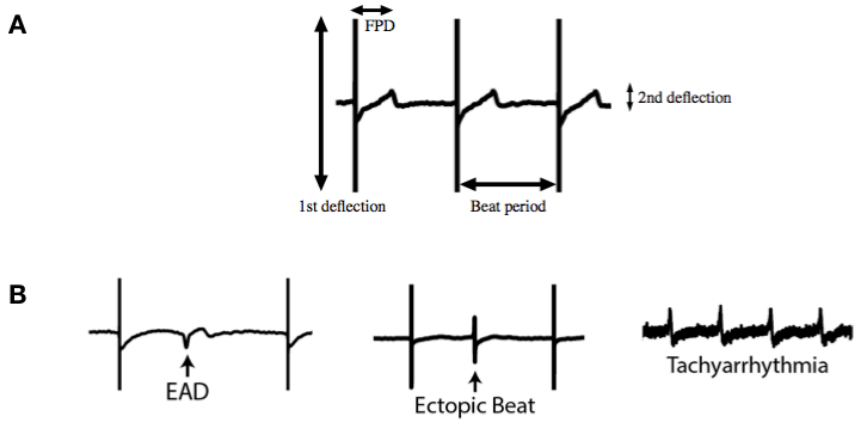

Figure 4 (A) Parameters of interest for the analysis of FPD recording with MEA. The 1st positive deflection displays the fast activation of voltage gated sodium channels, followed by a second, mostly positive, deflection which stands for the repolarization. The period between the great positive deflections is called the interspike interval or beat period, marked as RR on an ECG. The FPD is defined as the period between the first deflection and the top of the second deflection in one beat period. (B) Three possible arrhythmic configuration of MEA recorded FP in spontaneous beating CMs after incubation with proarrhythmogenic drugs or arrhythmia-inducing stimuli are shown in panel B. EADs are defined as one ore more positive or negative deflection in the interval of the second deflection. Ectopic beats have the same shape as normal beats but occur in the interval of the second deflection, thus a repolarization can not be safely distinguished from an ectopic beat. Tachyarrhythmia is characterized by tachycardia beating frequency of > 100 bpm with a reduced deflection amplitude. Mostly,

tachyarrythmias develop into a beating arrest in in-vitro analyzed CMs. EADs and ectopic beats can not be differentiated in tachyarrhythmic MEA recordings.

2.6.2. Patch clamp analysis

For patch clamp analysis matured LQT.3 CMs were washed with PBS w/o Ca/Mg and trypsinated (0,1 % Trypsin) to dissociate cells from long-term cultures (figure 3). LQT.3 CMs were seed at a low density of $5x10^4$ cells/mm^2 to ensure single-cell attachment. Cells were cultured in CM culturing medium. The measurements were performed 48 hours after dissociation on beating single-cells.

Manual patch clamp was performed using an amplifier (Zeiss-MCS Setup), pipette puller (Sutter Instrument CO.), micro-manipulator and patch clamp digitizer (Zeiss-MCS Setup) combined with a Zeiss-microscope. The membrane and action potential was measured using the whole cell configured patch clamp method. For measurements cells were washed with PBS and loaded with the external patch-clamp solution containing (in mMol/L) 140 NaCl, 4 KCl, 1,3 $CaCl_2$, 1 $MgCl_2$, 10 Hepes, 11 d-glucose with a pH of 7,4 adjusted with NaOH [30]. The internal solution used in patch-clamp analysis contained (in mMol/L) 4 NaCl, 115 potassium aspartat, 15 KCl, 1 $MgCl_2$, 2 NaATP, 3 MgATP, 5 Hepes, 10 EGTA with a pH of 7,2 adjusted with KOH. Both solutions were prepared using ultra pure water (18,3 μOhm at 24°C, 20 μM Ca^{2+}). The remaining Ca^{2+} in the ultra pure water gives the need to buffer Ca^{2+} with EDTA and EGTA [31]. Cells were kept at RT during the patch clamping with a equilibration time of 60 minutes in fresh CM culturing medium before measurement in the incubator at 37°C and 5% CO. Pipettes used for the patching were connected to a programmable micropipette puller and had resistances of 4 - 6 μOhm. The Ag/AgCl electrode was re-chloridized and the salt bridge containing 3 Mol/L KCl in agar was refreshed to prevent serial resistant and voltage clamping errors [32].

Data were recorded using MCS PC plotting software (MCS) and analyzed with the same tool**.** Recorded data included APD, resting membrane potential (RMP), AP amplitude (APA) and upstroke velocity. To distinguish cells in atrial-, ventricular- and nodal-like CMs, APD_{50} (APD at 50% of the repolarization curve) and APD_{90} (APD at 90% of the repolarization curve) were calculated. The APD_{90}/APD_{50} ratio can provide information over the characteristics of the CMs. APD_{90}/APD_{50} ratios of $\geq$ 1,8 points toward a fast phase-I repolarization, which is known to be characteristic for atrial-like CMs. A ratio $<$ 1,3 is characteristic for ventricular-like CMs witch a prolonged plateau phase. Intermediate ratios ranging from 1,3 - 1,7 are described as nodal-like cells [46]. Moreover the shape of the AP recorded with the patch clamp technique can indicate the structural role of the CM. An AP with prolonged plateau phase with steady increase of RMP before fast depolarization is designated as ventricular-like AP, whereas a fast depolarization from RMP with a short plateau phase and steady repolarization is designated as atrial-like AP. Nodal-like AP are characterized by fast depolarization and fast repolarization. The three different action potentials are shown in figure 5.

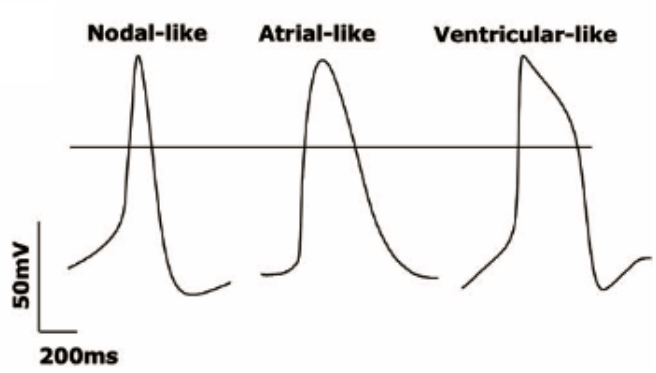

Figure 5 Characteristic AP curves showing the diversity of cardiac differentiation into atrial-like, ventricular-like and nodal-like CMs. The classification is based on the shape of the AP and on the APD_{90}/APD_{50} ratio (< 1,3 ventricular-like, 1,3 - 1,7 nodal-like, > 1,8 atrial-like) [46].

2.6.3. Impedance measurements

NSP 96-well culture plates (Nanion Sensor Plates CardioExcyte 96 - Stim-Type standard with extra stimulation electrode, order # 201003) were filled with PBS w/o Ca/Mg to measure base impedance as reference value followed by a fibronectin coating for 3 hours in the incubator. LQT.3 CMs were plated at a density of 30.000 cells/well in 200 μL CM culturing medium and incubated for 5 days on the CardioExcyte (Axion, Germany). Medium was changed twice daily by aspirating 50 μL for four times to prevent damage of the cellular syncytium.

Base-impedance, beating frequency and beat-rate-regularity index (BRRI%) as well as the peak-width 30% and 50 % were recorded with CardioExcyte Control software. Sweeps consisting of 10 seconds measuring interval were performed five times per hour over five days. Only wells with a stable base impedance amplitude of > 4 μOhm were used for data analysis. We used a 96-well formate for long-term analysis on the CardioExcyte to evaluate the beat rate regularity.

2.6.4. Calcium cycling measurements

Corning® 96 μcell plates with clear bottom were coated with fibronectin and incubated for three hours at 37°C and 5 % CO_2. LQT.3 CMs were seeded at a density of 30.000 cells/well and cultured for 3 days before measurements. One hour before dye loading medium was changed with 100 μl/well serum-free Tyrode's salt solution (Sigma-Aldrich) + 10 mM HEPES and 4,2 mM K^+ (Tyrode++, 1M potassium chloride solution, Sigma Aldrich). After equilibration 25 μl medium was taken off and 25 μl of 9 μM Cal-520 solution (abcam, ab171868) in Tyrode's buffer was added and incubated for 60 min. Then, medium was completely exchanged to a final volume of 90 μl/well Tyrode++. After a recovery period of 30 minutes in the incubator, the plate was transferred into the Hamamatsu Functional Drug Screening System (FDSS Hamamatsu, Japan) 7000EX and equilibrated for 10 minutes in the device before a baseline measurement was recorded. Subsequently 10 μL of tenfold concentrated compounds dissolved in Tyrode's solution were automatically added by the FDSS Hamamatsu 7000EX. Baseline parameters were beat rate, amplitude of fluorescent units due to cellular calcium transients, raising and falling slope as well as calcium transients duration (CTD) 30/50/70/90. Baseline recordings were generated and analyzed with n = 96 whereas the tested compound were analyzed with n = 7 per

concentration. Mean FPD and frequency was calculated and corrected with standard deviation. Furthermore a student's t-test was performed to test the statistical significance.

Fluorescence imaging of LQT.3 CMs intracellular Ca^{2+} transients was performed with the FDSS/μCELL at 25 frames per second and 37°C. Measurements were taken after 5, 15 and 30 minutes of incubation without taking the plate out of the FDSS Hamamatsu.

2.6.5. Cardiac contractile force measurements

Force measurements were performed in 8 well plates (Cor.4CE, Axiogenesis) with a 3 μm thick elastic silicon membrane as bottom seal shown in figure 6. This technique measures the oscillation of the silicon membrane as changes in air-pressure in a closed chamber and deflection of the membrane by proximity sensors due to the contraction of a beating CMs monolayer. Using this unique technique, the change in contraction force can be evaluated as well as the frequency and the duration and slope of the contraction and relaxation. The Cor.4CE plate was coated with fibronectin and LQT.3 CMs were washed with PBS w/o Ca/Mg and trypsinated (0,1 % Trypsin) to dissociate cells and seeded in 300 μL of CM culturing medium at a density of 3 x 10^5 cells per well. Medium was changed daily and volume was increased to 500 μL after two days.

Compound tests were performed with a 5 x stock concentration to ensure a sufficient dilution and incubated for 5 minutes on the analysis machine to avoid irritating or damaging stimuli to the silicon membrane. Compounds were measured for 30 seconds and beating behavior was averaged for each well using Cor.4CE-tool (Axiogenesis, Germany). Drug effects were tested with n = 2 per concentration. Mean FPD and frequency was calculated and corrected with standard deviation.

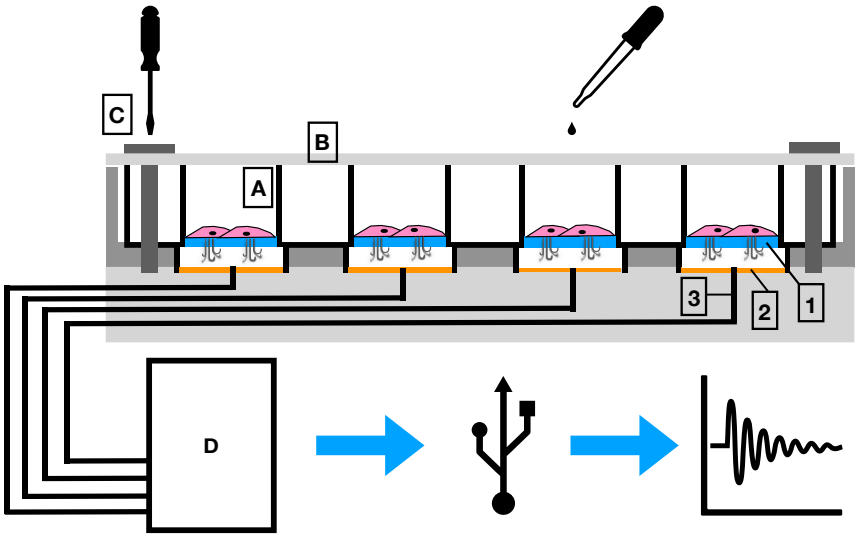

Figure 6 Cor.4CE setting in a 8-well format. The cover plate (B) of the wells (A) is fixated on the machine by screws (C) to ensure a stable ambient pressure in the space generated through the silicon membrane at the lower bottom of the 8-well (1) and the pressure sensor (2) of the Cor.4CE machine. The change in pressure in the space between the silicon membrane (1) and the proximity sensor (2, 3) is measured in (D) and recorded with a computer. Data is then generated as the change in amplitude over time as well as frequency, contraction and relaxation duration and slope. Compounds can be administered without great manipulations.

2.6.6. Compounds used for pharmacological studies

The drugs listed in table 1 were dissolved at stock concentration at 1000 fold concentrated compared to the highest concentration used for compound tests to ensure low vehicle concentrations. Ion-free sterile water, PBS w/o Ca/Mg and dimethyl-sulfoxid (DMSO, Sigma Aldrich) were used as vehicles. Compounds were administered as shown in figure 7.

Table 1 Drugs used for pharmacological experiments in LQT.3 CMs and Cor.V4U CMs

Drug	Concentration	Properties	Source
Ranolazin	1 - 3 - 10 - 30 µM	$I_{Na,L}$-Blocker	Tocris
Mexiletine	1 - 3 - 10 - 30 µM	I_{Na}-Blocker	Sigma-Aldrich
Dofetilide	1 - 3 - 10 - 30 nM	hERG-Blocker	Tocris
Ivabradine	0,01 - 0,1 - 1 - 10 µM	I_f-Blocker	Tocris
Sotalol	1 - 3 - 10 - 30 µM	ß-Blocker and hERG-Blocker	Sigma-Aldrich
Moxiflaxacin	3 - 10 - 30 - 100 µM	Antibiotic - Fluorquinon	Sigma-Aldrich
Nifedipin	1 - 3 - 10 - 30 nM	Ca^{2+}-Antagonist	Tocris
Verapamil	1 - 3 - 10 - 30 nM	Ca^{2+}-Antagonist	Sigma-Aldrich
Isoprenaline	0,1 - 0,3 - 1 - 3 - 10 - 30 - 100 - 30 nM	Mixed ß-agonist	Sigma-Aldrich
E-4031	1 - 3 - 10 - 30 nM	hERG-Blocker	Tocris
DMSO	0,00%, 0,01%, 0,05%	Verhicle	Sigma-Aldrich

Drugs and their tested concentration in hiPSC derived LQT.3 CMs and CorV.4U within this experimental setting. Properties of each drug and the source are also mentioned.

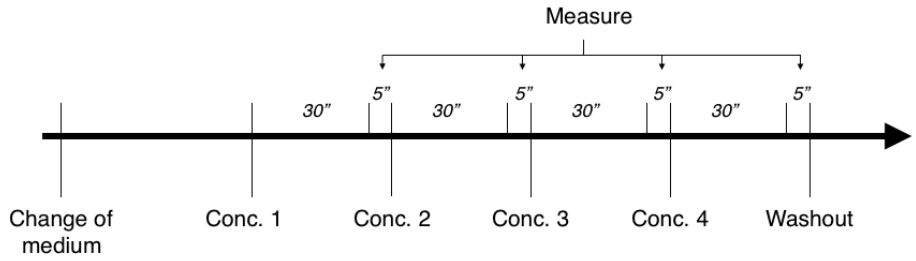

Figure 7 Time schedule for compound measurements. Each concentration was incubated for 30 minutes and cells were equilibrated in the incubator at 37,5°C and 5 % CO_2 whereupon measurement of 2 minutes took place on MEA, impedance, calcium cycling and contractile force measurement with 5 minutes incubation on the measurement machine. After the fourth concentration, compounds were washed out and fresh CM culturing medium was added.

3. Results

3.1. Genetic analysis of LQT.3 hiPSC

HiPSCs were tested by Coriell (USA) [27] for the expression of embryonic gene products necessary for iPSC transformation, which revealed a negative result for the embryonic genes (Oct-4, SOX-2, Nanog, GDF3, REX01). Karyotype analysis revealed a 46,XX karyotype with no structural chromosome aberration. Furthermore > 80 % of hiPSC stained positive for the SSEA-4. Splice site analysis of protein encoding exons as wells as comprehensive open reading frame carried out with polymerase chain reaction (PCR) and DNA sequencing of genomic DNA from the donor was performed by Coriell. A de novo mutation in the SCN5A gene (1218C>A, N406K) was detected by sequencing. The mutated gene was regularly expressed in hiPSC and differentiated CMs integrated the mutated ion channel in the sodium cycling.

3.2. Differentiation and culturing of LQT.3 cardiomyocytes

LQT.3 iPSC grew to a confluently monolayer of cells with a clear hiPSC-like morphology within 3 days (figure 2 and figure 8). Before differentiation was initiated hiPSCs were passaged three times to increase the amount of cells. HiPSCs started adherent differentiation in absence of Rock inhibitor and lacking the differentiation-inhibiting passaging. After addition of Chir990021 cells were directed to a cardiac differentiation pathway. Canonic WNT-inhibition increased this effect. Protein supply and growth factors were raised by addition of ßFGF (5 ng/mL) and 0,1 % HSA. On day eight, cells began to show spontaneous beating. The right panel in figure 8 shows a light microscope picture of an unpurified CM culture on day 10. The arrows point on round shaped CMs with one or more nuclei. After purification with puromycin, CMs were pooled and cells showed a stable beating activity. Purification was repeated two times to ensure the absence of non-cardiac cells. CMs grew in different morphologies as with sharp boarders, poly-angular, round, or trapezoid.

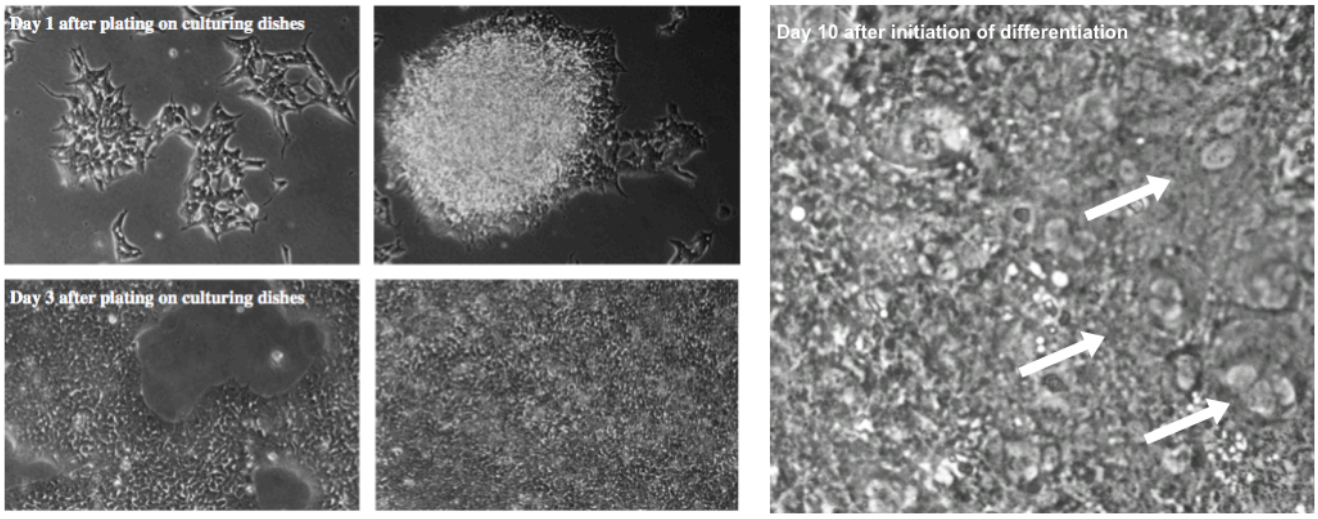

Figure 8 iPSC morphology is shown after 1 day and 3 days of platings cells. Cells grow confluently together and directed into cardiac differentiation. On day 10 the vast majority of cells show spontaneously beating activity.

3.3. Immunofluorescence analysis of LQT.3 cardiomyocytes

Cardiac-specific intracellular proteins and their three-dimensional organization within LQT.3 CMs grown in monolayer were visualized by immunofluorescent antibody staining. Matured LQT.3 CMs (> 8 weeks post differentiation and purification) stained positive for myosin light chain (MLC) 2V in figure 9 A, which is highly expressed in ventricular CMs [34]. Contrary the MLC2A, an atrial expressed myosin light chain, could not be detected in the LQT.3 CMs after two months of maturation (not shown in figure 9). Troponin (figure 9 B) and alpha-actinine (figure 9 D) could successfully be stained in the LQT.3 CMs due to a high expression rate in cardiac tissue. Connexin43 was shown to be highly expressed at the cell membrane as well as in the nuclear membrane (figure 9 E). CMs did not stain positive for Connexin40 which is expressed at the same locations as Connexin43. MLC-2V and troponin organized in myofilament-like structures. Alpha actinine is homogeneously distributed in the cell in longitudinal filaments. An overlay of MLC-2V and troponin is shown in figure 9 C and an overlay alpha actinic and Connexin43 is shown in figure 9 F to demonstrate cell boarders. Figure 9 E and 9 F show polynuclear CMs. Cardiac nuclei are stained with DAPI and visualized in blue (except for figure 9 C where no nucleus stained positive in this part of the culture or the DAPI overlay was not performed). Different cell densities only influenced the amount of expressed Connexin43 at the cell membrane, which was slightly higher at a higher density of LQT.3 CMs.

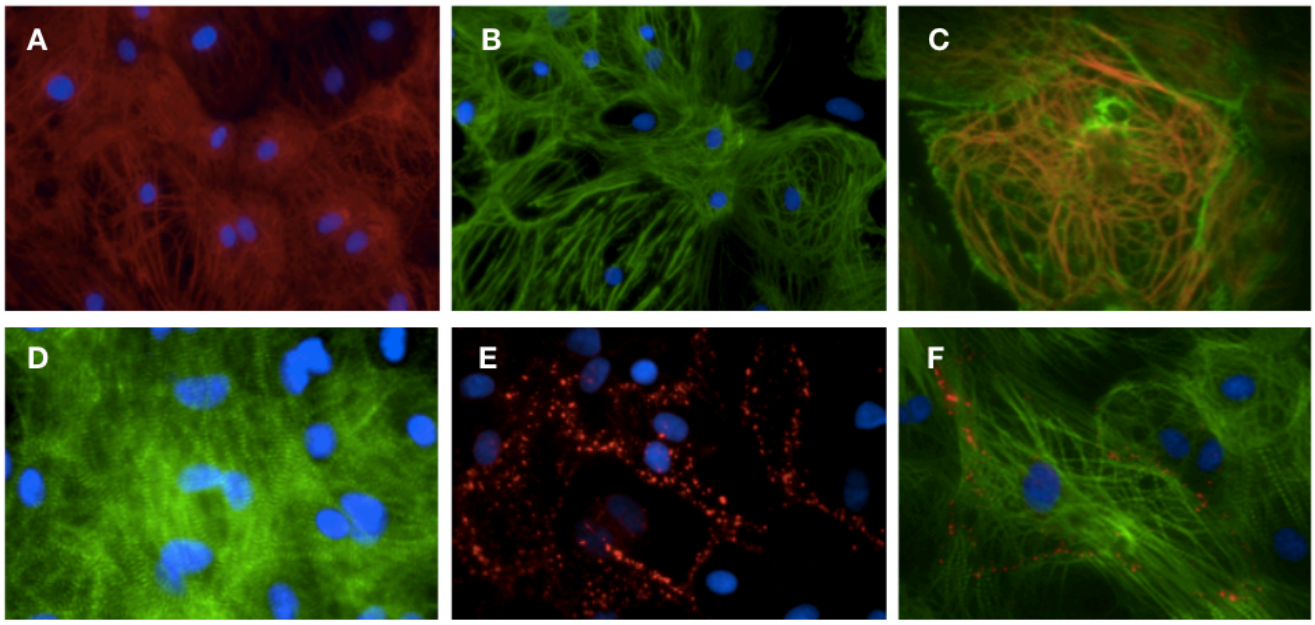

Figure 9 (A) LQT.3 CMs stained for MLC-2V (red), (B) Troponin (green) and overlay of both in panel C. DAPI staining is displayed in blue in all pictures. (D) LQT.3 CMs stained positive for Actinin (green), (E) Connexin43 (red), (F) overlay of Actinin and Connexin43.

3.4. Patch clamping of LQT.3 cardiomyocytes

General electrophysiological integrity of LQT.3 CMs was assessed with manual patch clamp analysis on single cells. The study revealed a maximum resting membrane potential of -65 mV and an amplitude of approximately 90 mV with a mean beat rate of 8,67 bpm. Figure 10 shows a AP of 1000 ms with a interspike interval of 5,7 seconds (10,52 bpm). The shape of the patch clamp AP implicating a prolonged plateau is characteristic for ventricular-like cells.

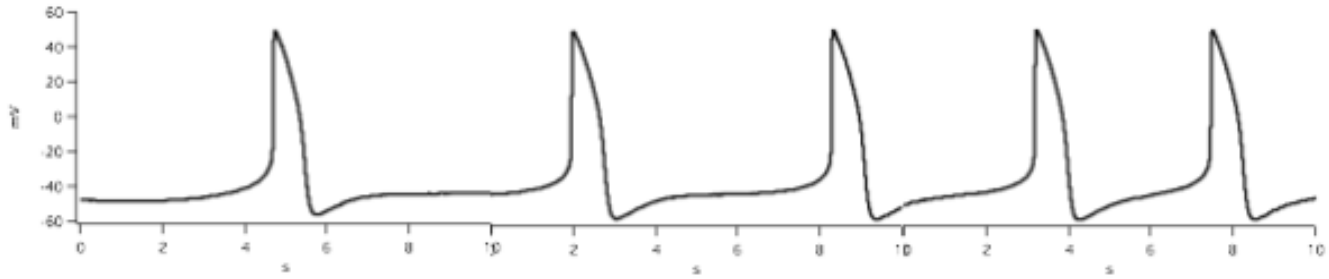

Figure 10 Action potential registration of LQT.3 CMs recorded with patch clamp analysis

3.5. Base impedance analysis of LQT.3 cardiomyocytes

Baseline impedance confirmed the prolonged AP in LQT.3 CMs in figure 11. Mean beat analysis revealed a mean beating interval of 560 ms (± 65 ms) after 4 days incubation on the NSP 96 well plate. The maximum base impedance amplitude in non-stimulated CMs was 4,9 mOhm with a beat rate of 53 beats/minute on day 4. The beat rate was slightly elevated on NSP plates in contrast to MEA plates. The beat rate regularity index (BRRI) of > 98% was reached after 30 hours and was stable afterwards. There were no significant beat rate variations recorded over 4,5 days.

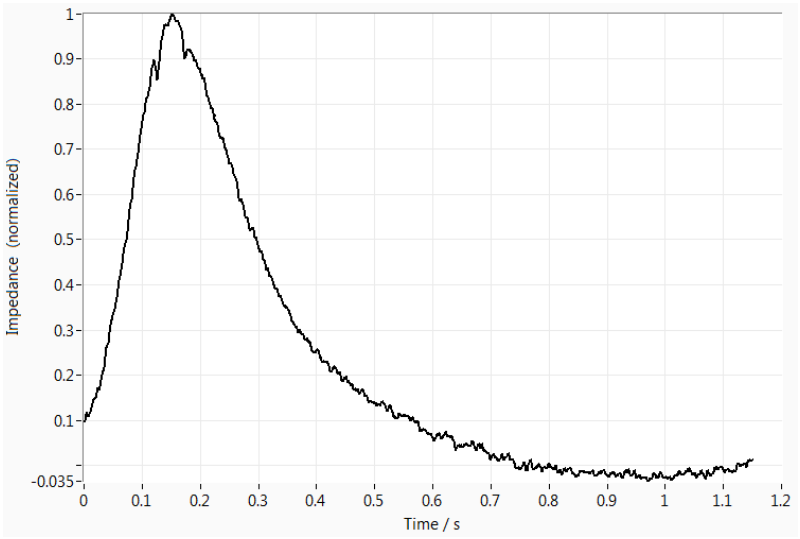

Figure 11 Mean beat of six beats of LQT.3 CMs recorded over a sweep period of 10 seconds. The graphic shows the prolonged APD of more than 500 ms resembling the LQT.3 phenotype. Base impedance measurement is useful to study long-term effects of medication. This measurement was taken after 4 days of incubation on NSP plates.

LQT.3 CMs showed a comparable base impedance implicating an adequate cell adherence on the culturing plate. Frequency was significantly lower in LQT.3 CMs compared to CorV.4U whereas peak width (PW 30) was significantly increased (table 2). The beat rate irregularity index was stable in both cell lines. Data from CorV.4U were used from El-Haou et al [38].

Table 2 Baseline impedance parameters of LQT.3 and CorV.4U CMs

Parameters	**LQT.3**	**CorV.4U**
Base impedance (Ω)	377 (± 6,4)	360,6 (± 4,1)
Frequency (bpm)	53 (± 1,0)	108,5 (± 1,0)
Amplitude (Ω)	4,9 (± 0,3)	3,6 (± 0,1)
PW30 (ms)	286,2 (± 0,8)	195,1 (± 1,0)

Impedance measurements are suitable for the evaluation of cardiotoxic ADR and the method of choice for long-term effects on cell viability. Base impedance and amplitude are the parameters of interest. Pro-arrhythmic effects can be studied using impedance measurement but it is limited to PW and BRRI. These parameters are not as appropriate as parameters in MEA and calcium cycling measurements.

3.6. MEA analysis of LQT.3 cardiomyocytes

QT-prolongation is one of the most feared cardiac side effects among new drug candidates but also among already existing and approved drugs. MEA measurements recording the FPD of CMs in-vitro correlate with the QT-interval in clinically recorded ECGs. Therefore, the FPD-influencing effect has a high impact on the prediction of the arrhythmogenic potential of tested compounds in in-vitro studies.

For baseline and compound FPD measurements, only FPs from LQT.3 CMs and reference Cor.4U CMs were used with a clear 'T-wave like signal'. Further exclusion criteria for FPs was a detection amplitude of $< 100\ \mu V$ for LQT.3 CMs and $< 300\ \mu V$ for CorA.4U and CorV.4U. Baseline ($p < 0{,}001$) and frequency corrected FPD, using the Bazett (FPDcB) correction formula ($p < 0{,}05$) and the Frederricia (FPDcF) correction formula ($p < 0{,}001$), were significantly increased in LQT.3 CMs than in CorA.4U CMs. FPDcB was significantly increased in LQT.3 CMs compared to CorV.4U ($p < 0{,}05$). Baseline measurements are summarized in table 3. Values are shown as standard deviations of mean FPD with a total number of averaged values used for the analysis of 80 values for LQT.3, 83 values for CorV.4U and 91 values for CorA.4U. RR is defined as the time interval between the two great positive spike deflections and measured in seconds.

$$FPDcF = FPD/\sqrt[3]{RR} \qquad FPDcB = FPD/\sqrt{RR}$$

Equotation 1 Frequency adjusted field potential duration using Frederricias' (FPDcF) and Bazett's formula (FPDcB).

Table 3 Frequency adjusted FPD in LQT.3, CorV.4U and CorA.4U CMs

Parameters	**LQT.3**	**CorV.4U**	**CorA.4U**
Frequency *(/min)*	22,58 (± 2,74)	62,28 (± 4,55)	100,99 (± 7,88)
FPD (ms)	603,79 (± 43,39)	278,30 (±70,91)	160,01 (± 25,98)
FPDcF (ms)	430,74 (± 60,91)	253,22 (± 41,65)	189,89 (±29,91)
FPDcB (ms)	370,88 (± 36,91)	253,77 (±106,65)	206,92 (± 32,37)
n (wells/96well)	80	83	91

3.6.1. Mexiletine effects in LQT.3 cardiomyocytes

The class Ib anti-arrhythmic drug (AAR) mexiletine acts as a sodium channel inhibitor which stabilizes the membrane potential and shortens the action potential. Mexiletine is known to have a weak effect if it is used alone. For this reason, mexiletine is often combined with chinidine, sotalol or procainamid. Instead of a FPD-shortening, a dose-dependent prolongation of FPD from 22,14 % to 36,04 % was detected with a reduction of this dose-dependent prolongation of FPD at 30 μM to 22,65 % seen in figure 12. Furthermore a reduction of the dose-response increase of FPD after 30 minutes incubation time at 1, 3 and 10 μM (3,95 % to 9,39 %) and a further increase of the dose-dependent prolongation of FPD at 30 μM to 48,93 % was observed. Mexiletine revealed a decrease of frequency after 5 minutes incubation time starting at 1 and 3 μM and an slight increase of frequency at 30 μM. Frequency increased after 30 minutes incubation time at 3 and 10 μM with a decrease of frequency at 30 minutes incubation time at 30 μM. Compared to CorV.4U, a prolongation of FPD was not detected but a decrease in frequency.

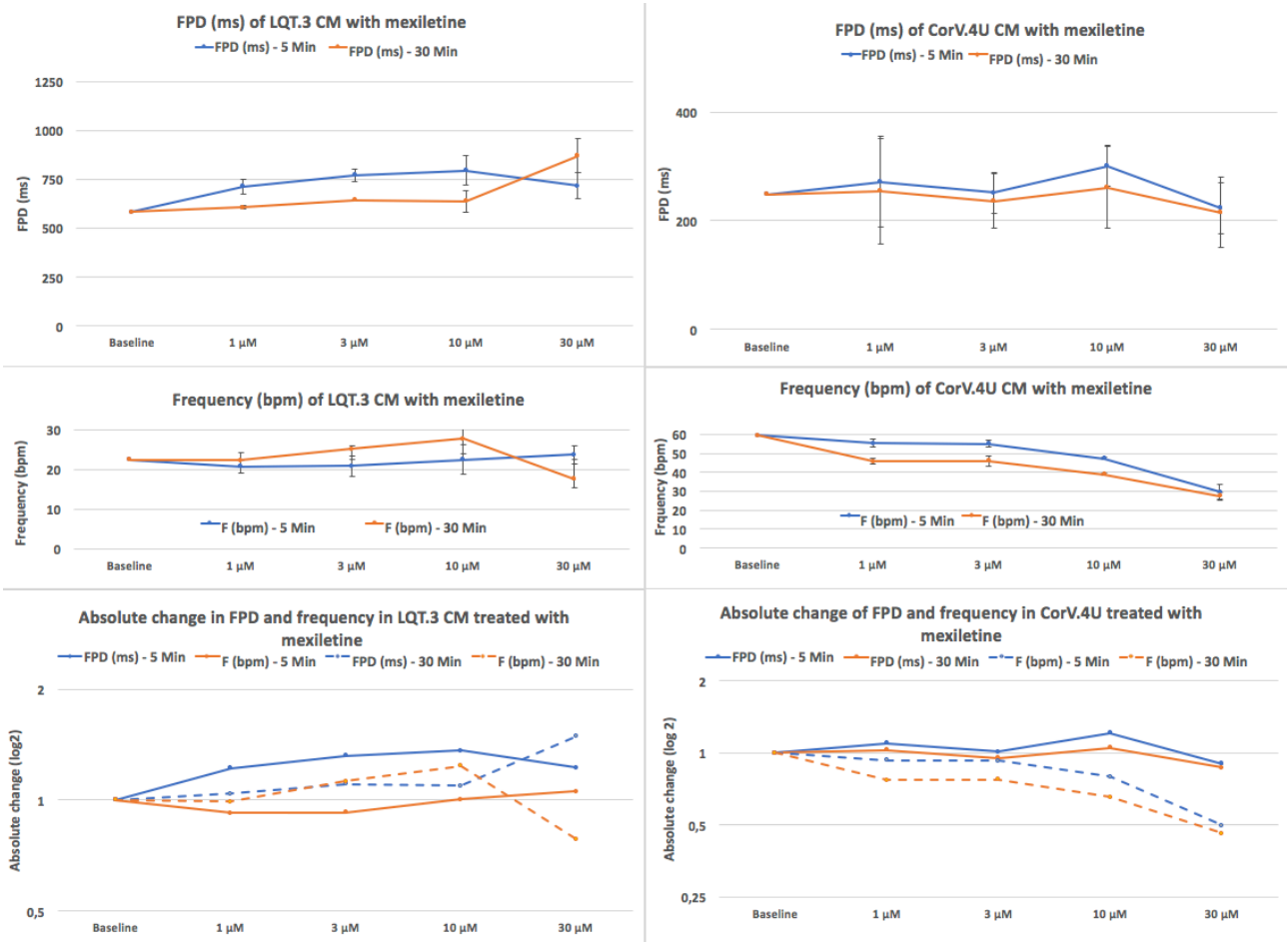

Figure 12 The effect of mexiletine shows a dose-dependent prolongation of FPD and decreasing of frequency.

3.6.2. Ranolazine effects in LQT.3 cardiomyocytes

LQT.3 CMs showed a dose-dependent prolongation of FPD to ranolazine. This drug acts as an antagonist of the $I_{Na,L}$ and sodium-dependent Ca^{2+} channels on the surface membrane of CMs. This decreases inward calcium current and promotes the relaxation during the diastole (positive lusitrope). Furthermore, ranolazine has an inhibitory effect of the outward rectifying potassium current by

blocking this channel [14]. We detected a prolongation after 5 minutes incubation of 35,1 % to 88,3 % with a diminishing of this dose-dependent prolongation of FPD after 30 minutes incubation of 15,97 % to 31,13 % as shown in figure 13. We observed a shortening of the beating frequency at 5 minutes incubation time starting at 3 μM (20 bpm) and further shortening 10 μM (17,5 bpm) with a steady frequency at 30 μM (17,25 bpm). In contrast to the 5 minute incubation, the 30 minutes incubation showed an increase in frequency with 3 bpm and 1,6 bpm at 1μM and respectively 3 μM. To the contrary, the FPD was not prolonged in CorV.4U CMs but the frequency was significantly decreased.

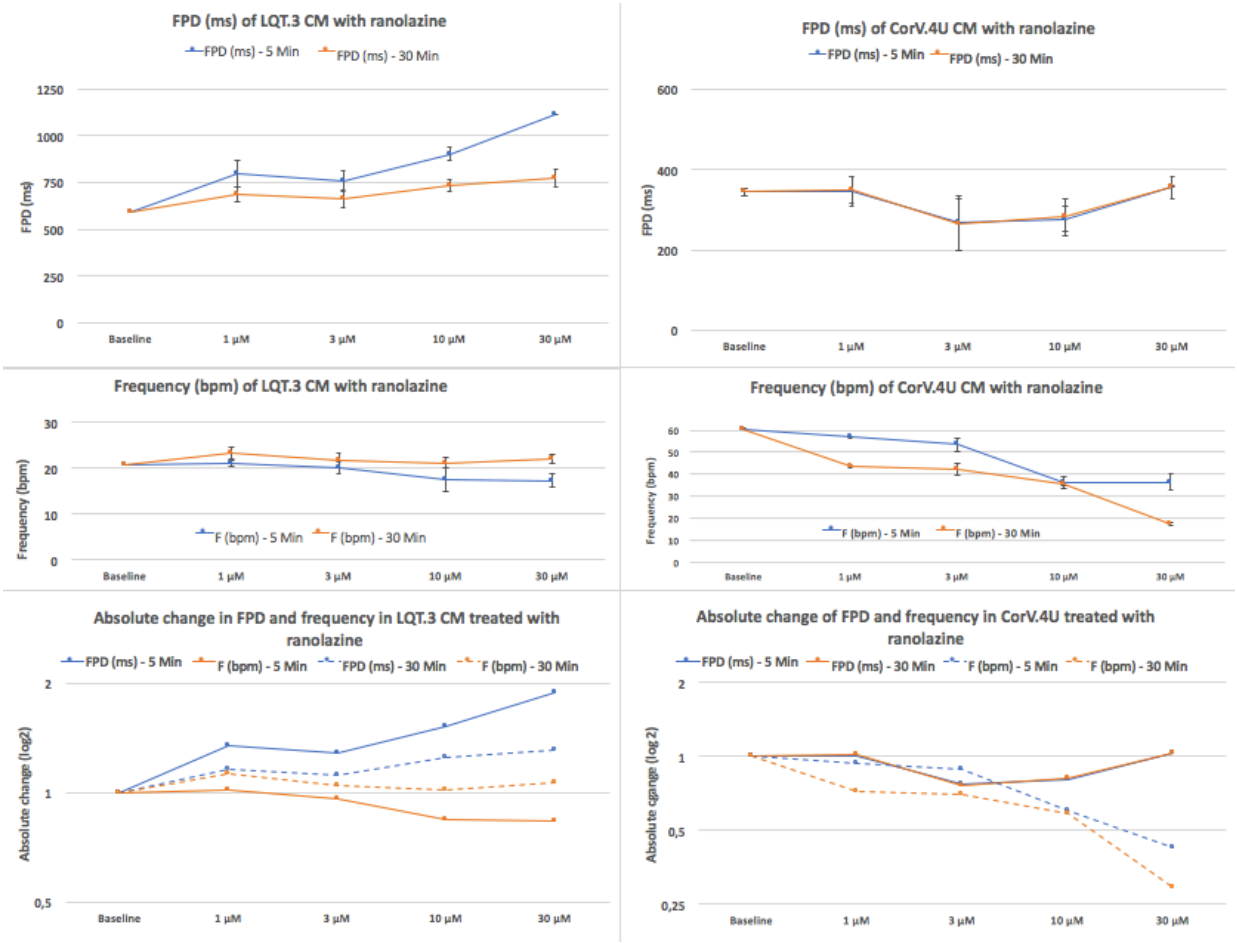

Figure 13 LQT.3 CMs reacted to a challenging with ranolazine with a prolongation of FPD in lower doses together with a decreasing of this prolonged FPD at higher doses.

3.6.3. Sotalol effects in LQT.3 cardiomyocytes

Sotalol is a mixed class II and class III anti-arrhythmic that affects CMs by inhibiting unselectively the ß$_1$- and ß$_2$-adrenergic adrenaline receptors. This leads to a negative inotrope and chronotrope effect of sotalol on CMs. Furthermore, the efflux off potassium is inhibited, which leads to prolonged repolarization and refractory period. LQT.3 CMs showed a dose-dependent prolongation of FPD after 5 minutes incubation (22,14 % to 36,04 %) as shown in figure 14. We detected an increase of the dose-dependent prolongation of FPD after 30 minutes incubation time at 3 and 100 μM in comparison to 5 minutes incubation time. Frequency was shortened after 5 minutes incubation time starting at 1 μM with an increase of frequency at 30 μM. In contrast to this significant increase in FPD, the FPD in CorV. 4U was also elevated but not as sensitive as the LQT.3 CM. CMs ended up in a beating arrest after 30 minutes of incubation under the highest concentration.

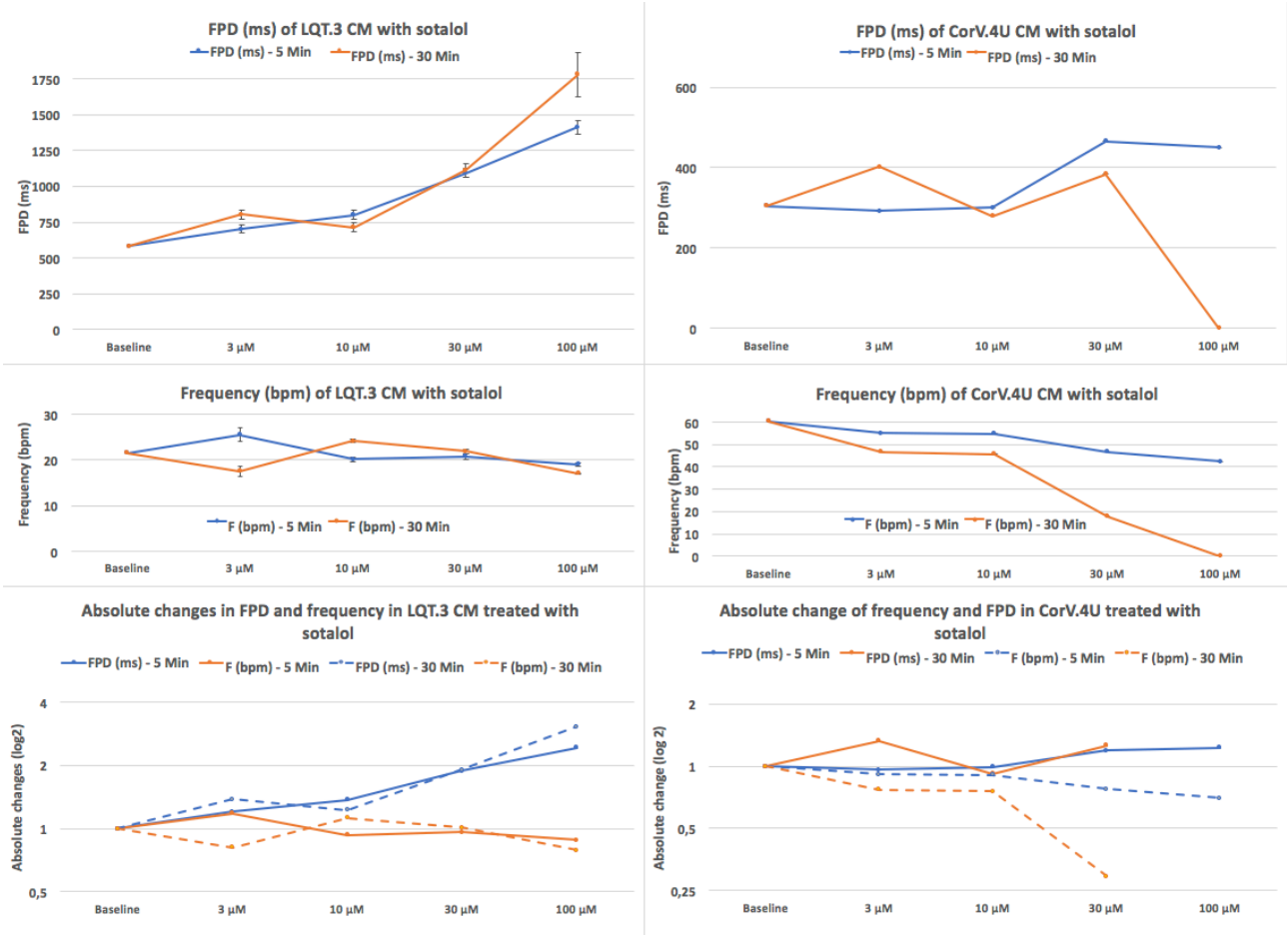

Figure 14 Sotalol revealed a prolongation of FPD, without inducing a beating arrest. Frequency was dose-dependently decreased.

3.6.4. Moxifloxacin effects in LQT.3 cardiomyocytes

Moxifloxacin, a fluoroquinolone antibiotic known for a QT-prolonging effect by unselectively blocking the hERG channel, revealed a dose-dependent prolongation of FPD at 5 minutes incubation time ranging from 24,89 % to 83,91 % with a diminishing of the dose-dependent prolongation of FPD at 30 minutes incubation time (5,13 % to 39,44 %). Figure 15 shows a light increase of frequency at 5 minutes incubation time at 3 μM and a dose-dependent shortening of frequency at 100 μM. Frequency was steady after 30 minutes incubation time. CorV.4U CMs did not respond as strong to moxifloxacin on FPD. Frequency was decreased slightly after 30 minutes of incubation.

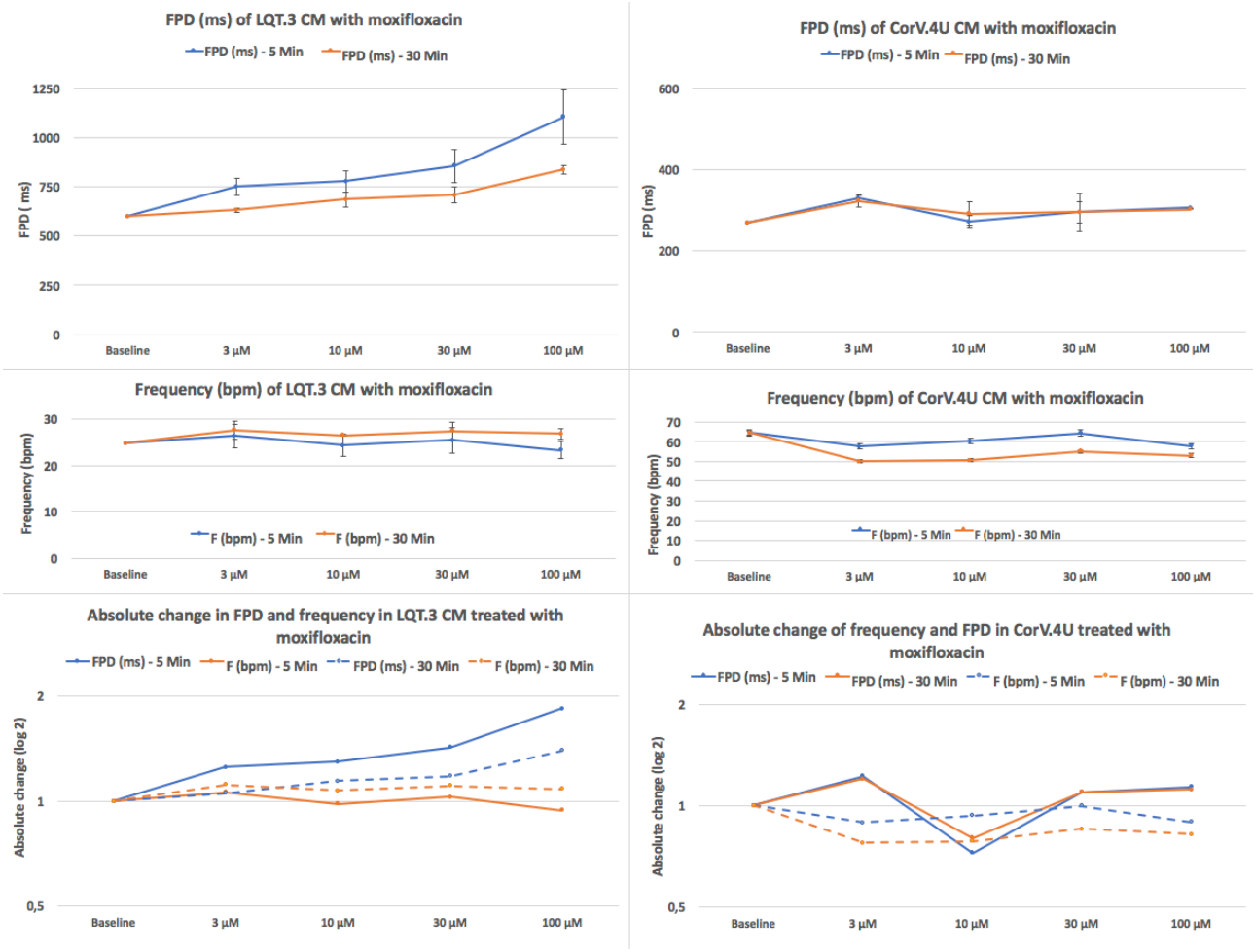

Figure 15 The fluoroquinolone moxifloxacin is known for its QT-prolonging effect. Also LQT.3 CMs showed a significant dose-dependent prolongation of FPD with a reduced frequency.

3.6.5. Ivabradine effects in LQT.3 cardiomyocytes

The I_f-channel is mainly expressed in the sino-atrial node and is responsible for continuous generation of APs. The channel can be blocked by the specific antagonist ivabradine. On the one hand this causes a slow depolarization of pacemaker cells leading to a reduced frequency and on the other hand a prolongation of the diastole. We observed a dose-dependent prolongation of FPD after 5 minutes incubation (25 % to 53 %). FPD prolongation was increased dose-dependently after 30 minutes incubation (35 % and respectively 62 %). Frequency was shortened after 5 minutes of incubation (figure 16). At concentrations of 1 μM and 10 μM ivabradine, no clear T-wave like signal could be detected on the CiPA tool after 30 minutes. Frequency could be calculated using the interspike-interval. FPD was linear elevated in CorV.4U with a total increase of 25 %. Frequency was decreased with 50 % after 30 minutes for the highest concentration tested.

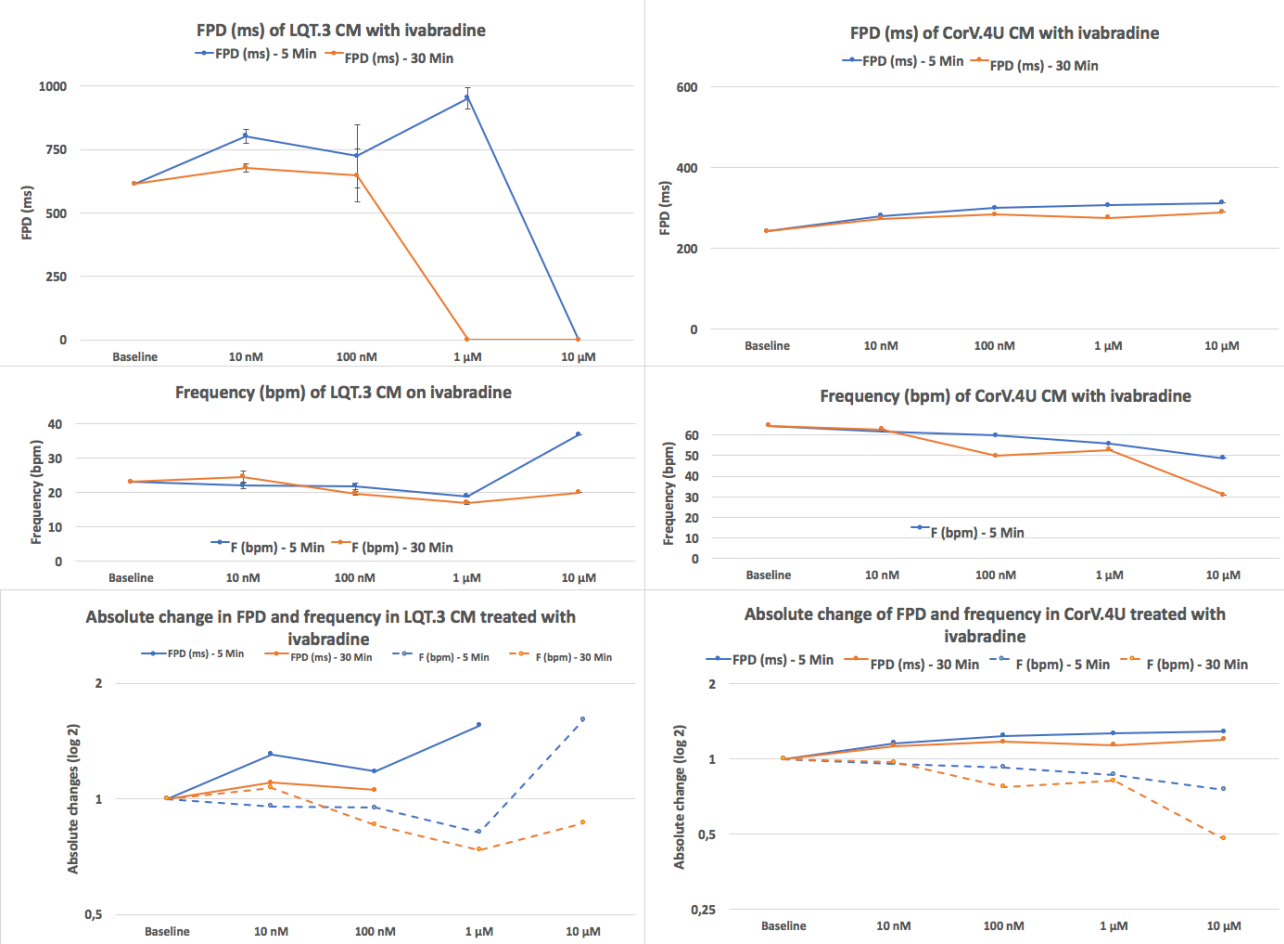

Figure 16 Ivabradine lead to strong increase in FPD and decrease in frequency.

3.6.6. Dofetilide effects in LQT.3 cardiomyocytes

Dofetilide is a class III anti-arrhythmic drug, which selectively blocks the rapid component of the delayed rectifier outward potassium current (I_{Kr}). Dofetilide has a known pro-arhythmic potential by a dose-dependent increase of the QT interval. On the one hand, the I_{Kr}-block is used in the treatment of atrial flutter and atrial fibrillation to prolong the refractory period of atrial tissue, while on the other hand physicians do not prescribe this drug frequently due to the high proarrhythmogenic potential. We observed a linear dose-dependent FPD prolongation after 5 minutes incubation at 3 - 30 nM (figure 17). After 30 minutes incubation time a diminishing of the dose-response increase of FPD was noted. Dofetilide showed a decrease of frequency after 5 minutes in a dose-dependent manner with a diminishing of dose-response decrease of frequency after 30 minutes incubation time at all doses. At a concentration of 30 nM, dofetilide induced a tachyarrhythmia in several wells of LQT.3 CMs which lead to a beating arrest graphically shown in figure 18. FPD was also dose-dependent elevated in CorV.4U but not as intense as in the LQT.3 CMs. Furthermore a beating arrest without any preceding arrhythmia was seen at 100 nM. No clear T-wave like signals could be measured at 10 nM and 30 nM after 30 minutes.

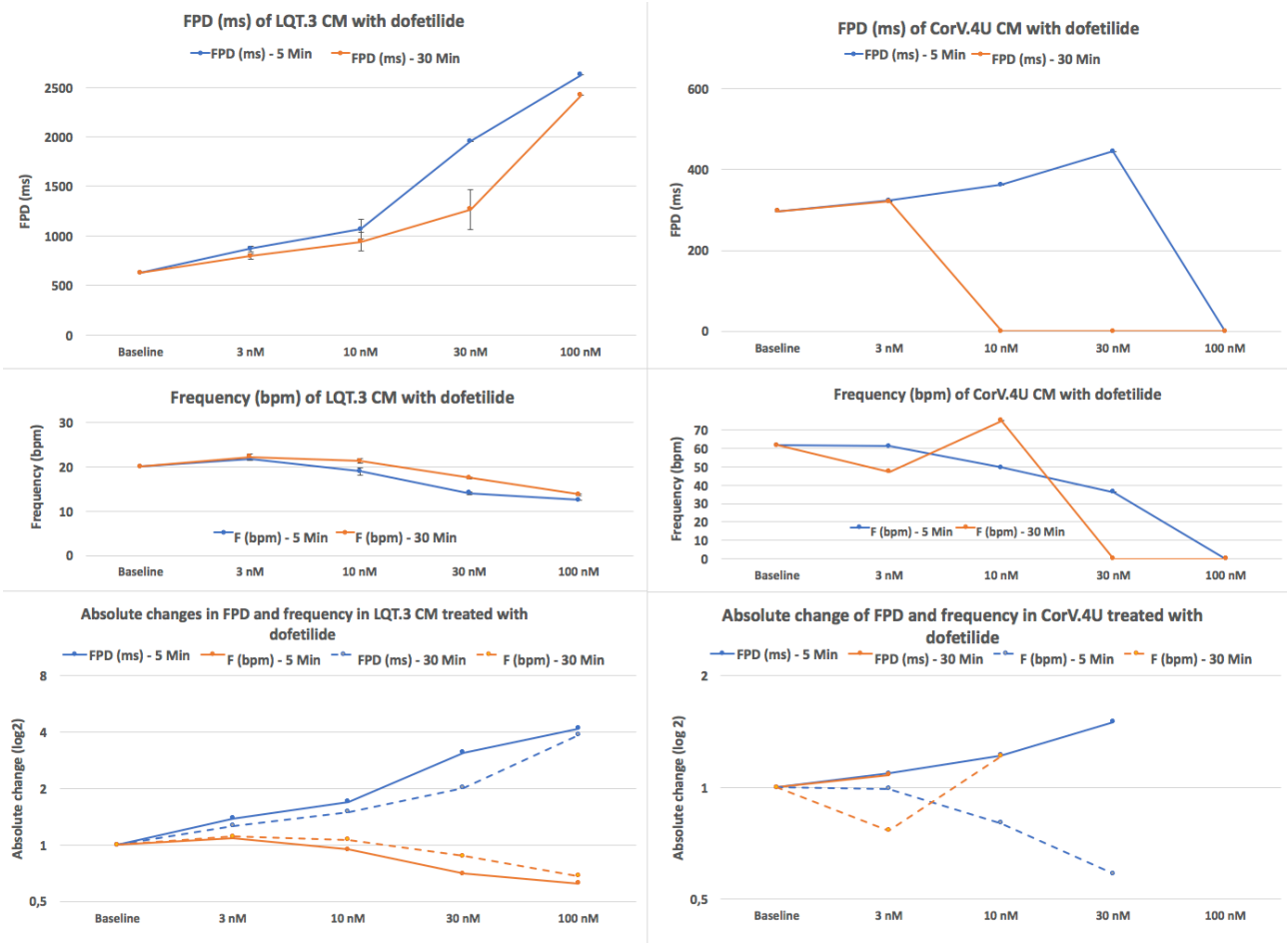

Figure 17 Dofetilide showed a strong FPD prolonging effect with a decrease of frequency.

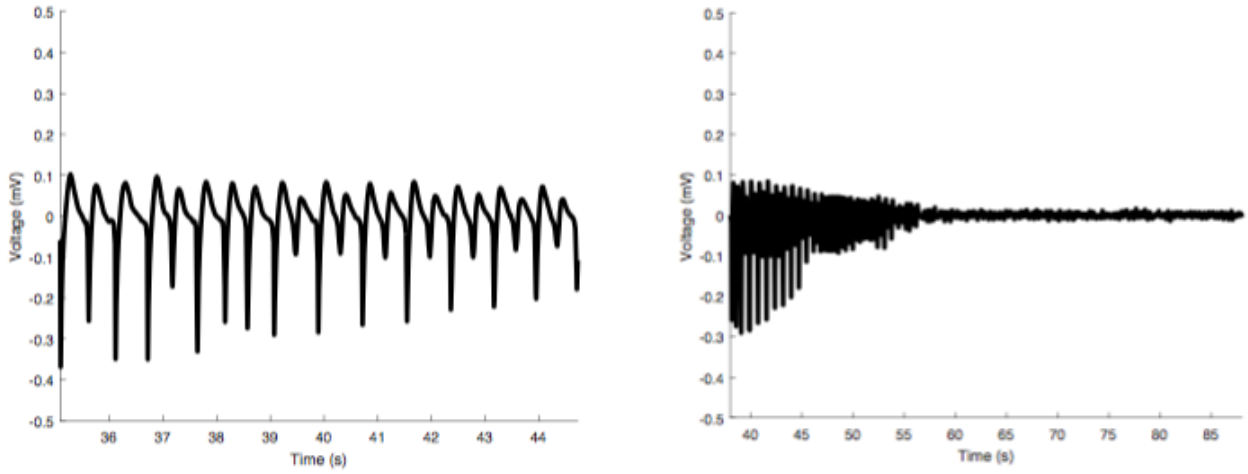

Figure 18 Arrhythmic events in LQT.3 cardiomyocytes beating behavior could be registered during MEA measurements with 30 nM dofetilide. The left panel shows a tachyarrhythmia with a frequency of 108 beats per minute. During this period a few ectopic beats occurred. Additionally, a reduction of FP-amplitude from 0,5 mV to a stable beating arrest within 30 seconds occured.

3.6.7. Nifedipine effects in LQT.3 cardiomyocytes

Nifedipine, a dihydropyridine-type Ca^{2+} channel blocker, showed a dose-dependent shortening of FPD as well as a dose-dependent increase of frequency starting from 1 nM to 30 nM (figure 19). In this setting only 5 minute incubation time was measured.

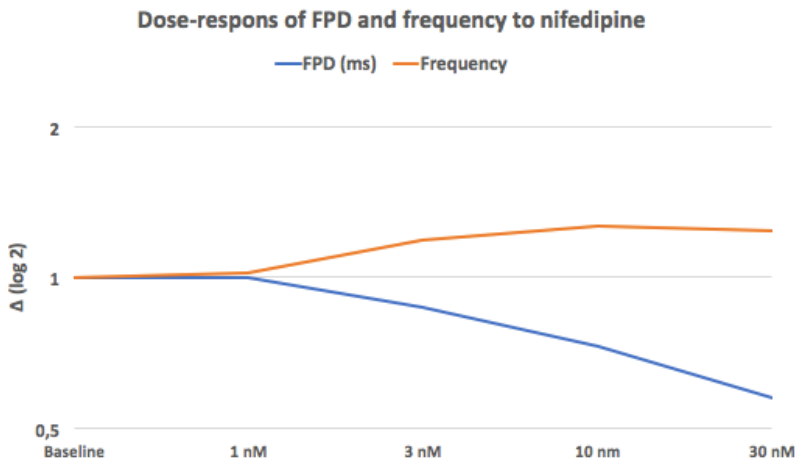

Figure 19 Nifedipine shows a strongly dose-dependent shortening of FPD and increasing of the frequency.

3.6.8. Isoprenaline effects in LQT.3 cardiomyocytes

To evaluate wether LQT.3 CMs respond to alpha-adrenergic catecholamines, we tested isoprenaline in the concentrations mentioned in table 1. Testings revealed a shortening of the FPD in a strong linear dose-dependent manner accompanied with a chronotropic effect (figure 20). Already small concentrations of 0,3 nMol/L reduced the FPD by 5,46 % reaching a decrease of FPD by 34,46 % at 300 nM isoprenaline.

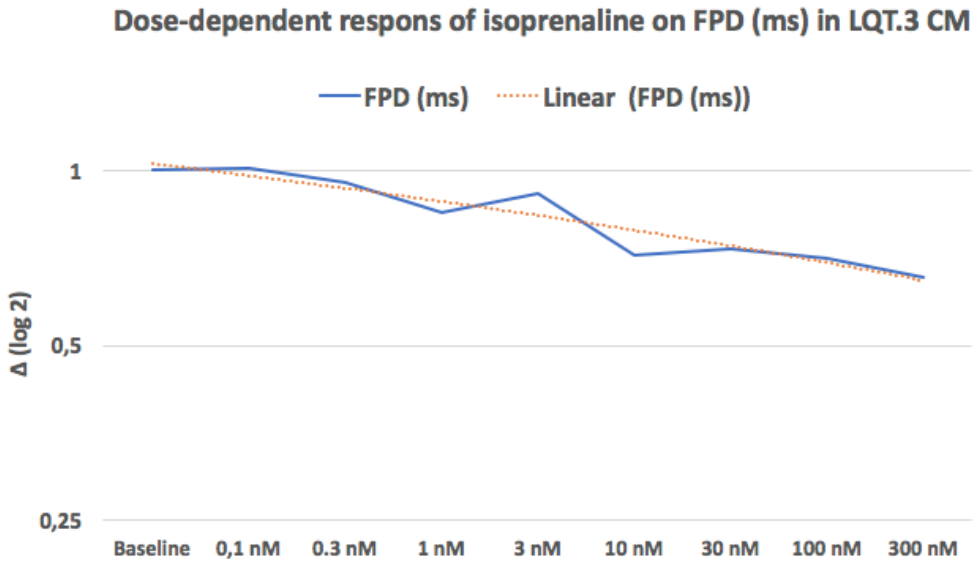

Figure 20 Linear dose-dependent decrease of FPD in LQT.3 CMs after challenging with isoprenaline

3.6.9. E-4031 effects in LQT.3 cardiomyocytes

As a second positive control E-4031, a hERG-channel blocker, was used. An increased FPD with a stable beating frequency (figure 21) was detected. Time dependent blockage of hERG channels with dofetilide was also seen in CorV.4U but not as sensitive as the LQT.3 CMs. CorV.4U CMs developed a beating arrest at 30 nM E-4031 after 30 minutes of incubation.

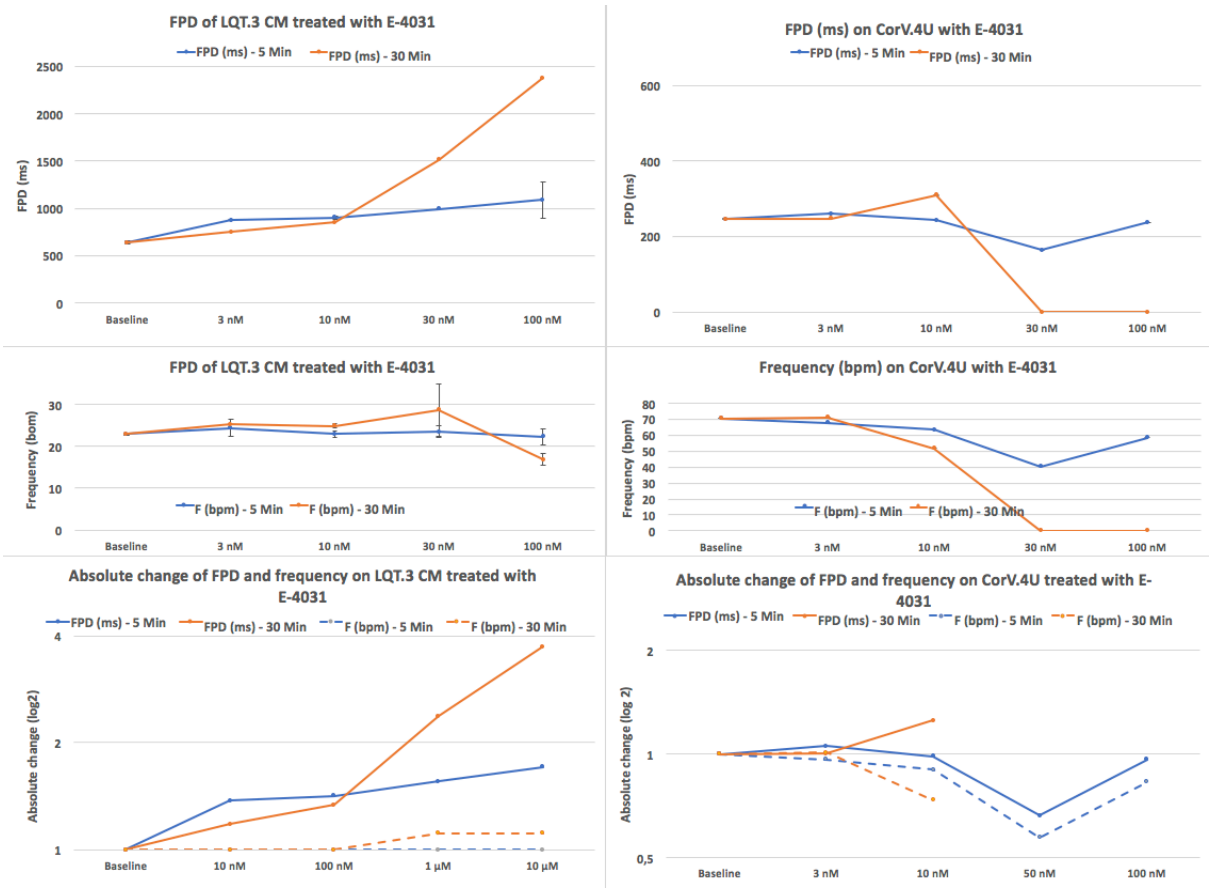

Figure 21 Behavior of LQT.3 CMs to challenge with the hERG-channel blocker E-4031

3.6.10. Arrhythmic events in LQT.3 cardiomyocytes

Spontaneous arrhythmic events were not registered spontaneously under baseline conditions on MEA plates. Arrhythmic events such as EADs, DADs, ectopic beats or tachyarrythmias could be induced by stimulating LQT.3 cells with potential proarrhythmogenic stimuli such as electrical up-pacing, catecholamine challenge such as isoprenaline, the Ca^{2+} releasing substance caffein or for example QT prolonging drugs such as dofetilide.

Administration of 10 mMol/L caffeine dissolved in PBS resulted in generation of EADs and DADs (left graphic figure 22). Escalating the caffein concentration to 20 mMol/L resulted in further EAD and DAD formation as well as ectopic beats and FP configurations of extrasystoles (right graphic figure 22).

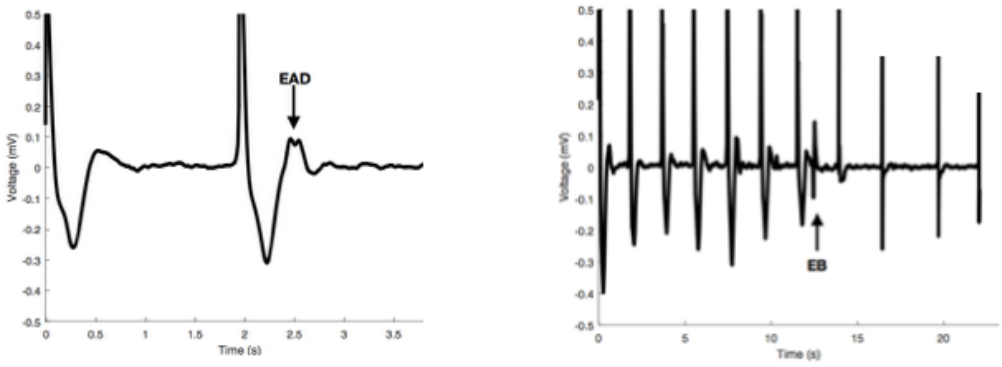

Figure 22 Arrhythmic events of LQT.3 CMs recorded during MEA measurements with 10 and 20 mMol/L caffeine. EAD in the left panel and ectopic beats in the right panel were seen.

LQT.3 CMs were electrically paced on MEA plates using one pacing electrode under control of AXiS software. CMs were paced at 60 bpm for 60 seconds to induce a relative tachycardia-like situation, representing the major risk factor for arrhythmic events in LQT syndrome type 3 patients. After 60 seconds of pacing cells spontaneously entered their rhythm of 31 beats per minute showing several arrhythmic events (figure 23). These arrhythmic events included disturbed repolarisation behavior and ectopic beats. EADs and DADs were registered after pacing with 120 bpm. Several EADs turned into rolling EADs and prolonged beating interval. By using electrical pacing, no beating arrest could be induced.

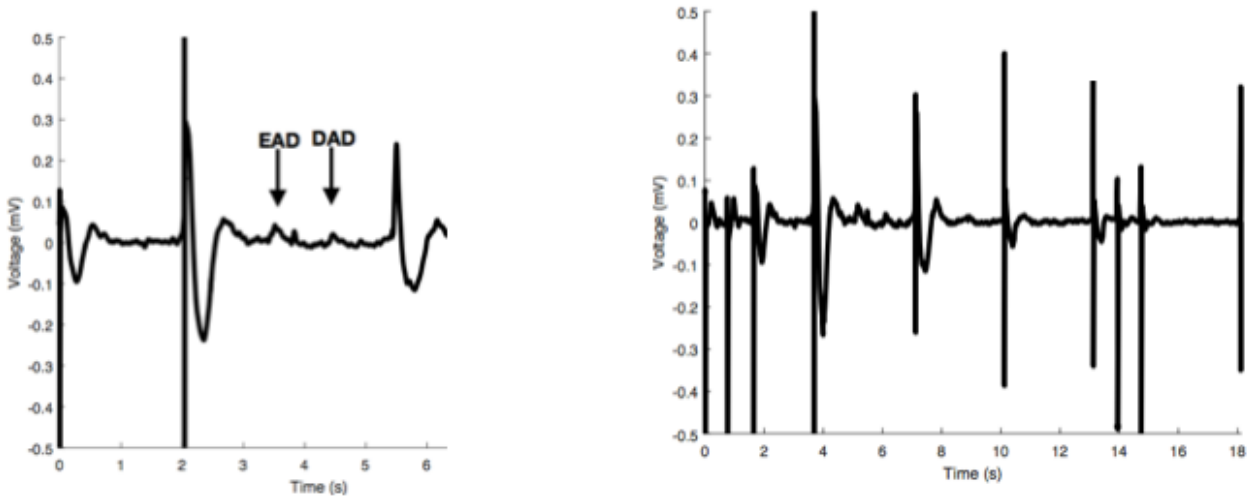

Figure 23 Electrical pacing of LQT.3 CMs with 1Hz and 2 Hz with Axion MEA systems control software revealed arrhythmic events. We see ectopic beats and repolarization disturbances.

3.7. Calcium cycling analysis of LQT.3 cardiomyocytes

Results were obtained from measurements at baseline conditions and after 5, 15 and 30 minutes of compound incubation on the FDSS Hamamatsu 7000EX. Here, data from an incubation time of 30 minutes is reported. Plates were incubated without any interaction except the fluorescence measurement at the defined time points. A sample size of n = 7 and control sample size of n = 2 was chosen. Statistical analysis was performed using a student's t-test with a cut of level $p < 0{,}05$.

3.7.1. Mexiletine and ranolazine effects in LQT.3 cardiomyocytes

Mexilitine showed a decreased beat rate as already seen on MEA experiments. Calcium transients duration after 30 % of the total calcium transients (CTD30) was not significantly changed, whereas CTD90 was raised with a factor 3. Spike amplitude was stable over time (figure 24).

Beat rate of LQT.3 CMs was dose-dependently reduced by ranolazine with an absolute beating arrest at 30 μM. Spike amplitude was constantly diminished during application of ranolazine (figure 24), but did not further decrease with higher concentrations. CTD30 and CTD90 increased both with 25% at 1 μM and 30% respectively 40% at 3 μM. At further concentrations of 10 μM ranolazine, CTD90 significantly raised with 240% whereas CTD30 was raised by 60%.

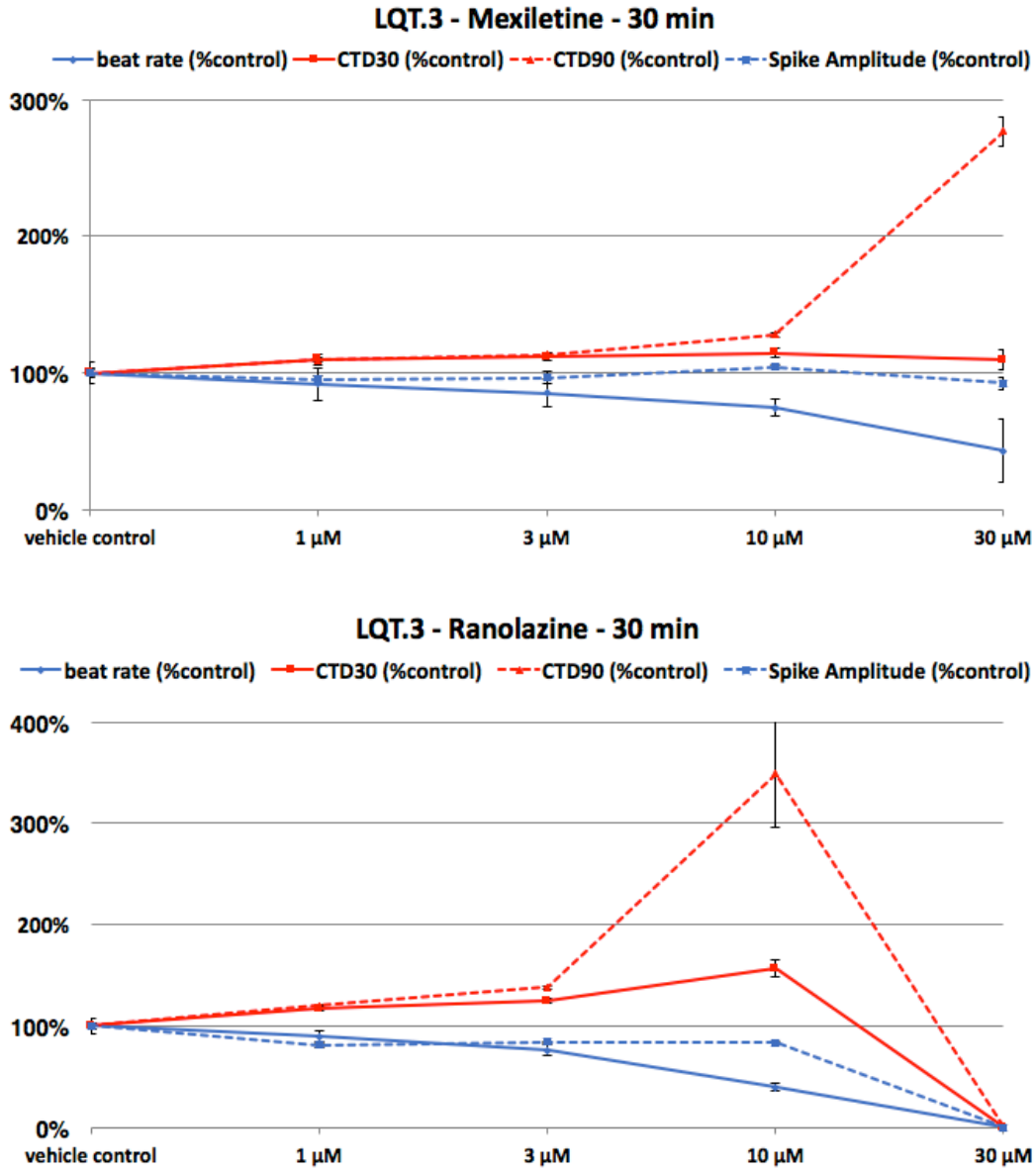

Figure 24 Calcium cycling of LQT.3 CMs showing beat rate, CTD30 and 90 and spike amplitude

3.7.2. Dofetilide and moxifloxacin effects in LQT.3 cardiomyocytes

Dofetilide affected LQT.3 CMs by a decreased beat rate and spike amplitude accompanied with a dose-dependent raise in CTD30 and CTD90 at 1 and 3 nM with a factor 3,8 (figure 25). CTD30 increased in at 10 nM dofetilide twofold to the baseline values. CTD90 increased to a tenfold increase at 10 nM.

The beat rate of LQT.3 CMs was slightly affected and decreased by 10% at moxifloxacin concentrations of 3, 10, 30 and 100 μM (figure 25). Spike amplitude increased ad 3 and 10 μM but decreased at higher concentrations. CTD30 and CTD 90 were increased by 10% at 3 and 10 μM. CTD30 slightly decreased to 5 % and CTD90 increased to 20% at 100 μM moxifloxacin.

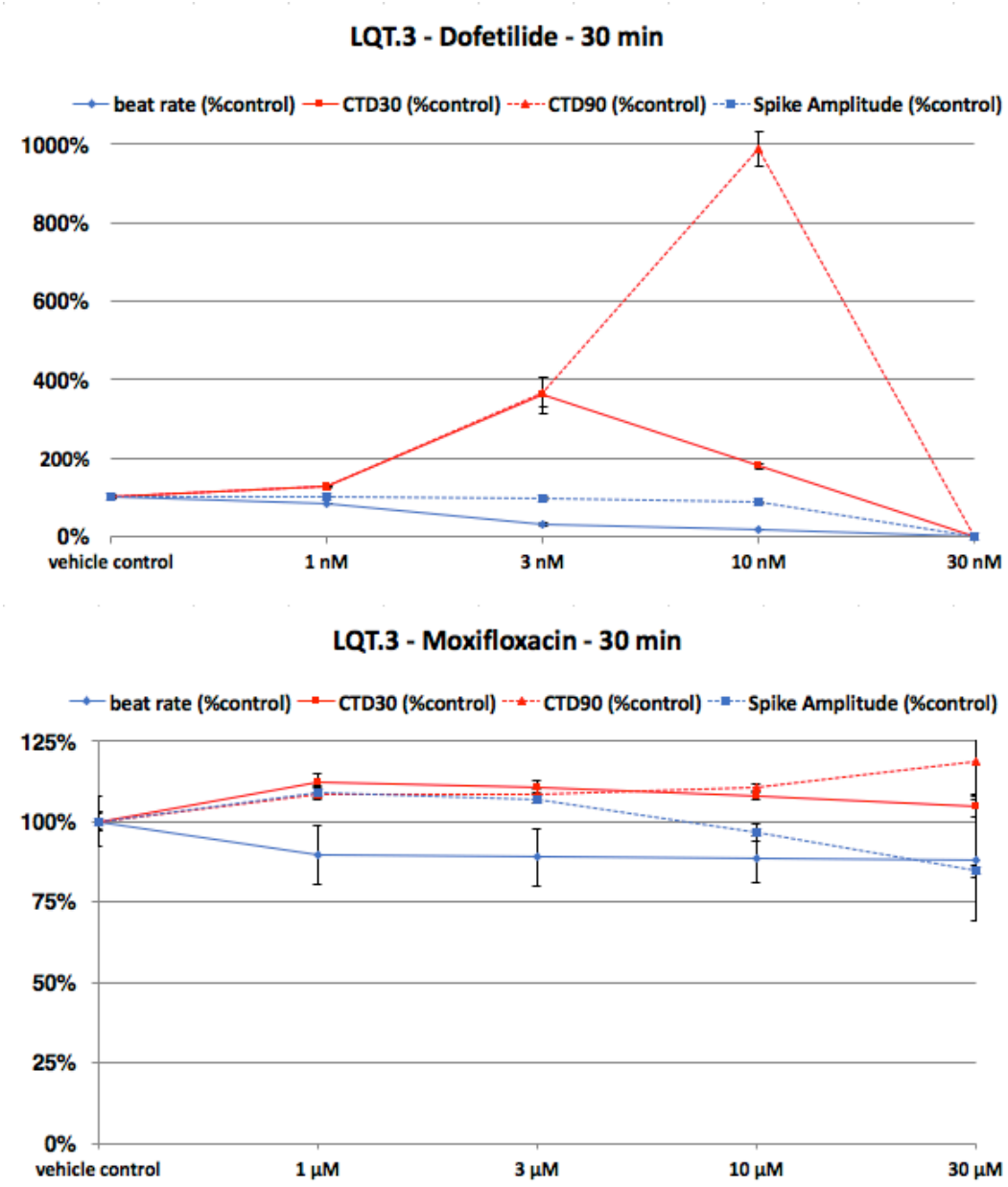

Figure 25 Calcium cycling of LQT.3 CMs showing beat rate, CTD30 and 90 and spike amplitude

3.7.3. Sotalol and ivabradine effects in LQT.3 cardiomyocytes

Sotalol administration revealed a decrease in beat rate and an absolute beat arrest at 100 μM after 30 minutes of incubation (figure 26). CTD30 raised linear to 270% compared to baseline conditions. CTD90 increased sixfold compared to baseline measurements.

Beat rate and Spike amplitude were both dose-dependently diminished by ivabradine (figure 26). CTD30 and CTD90 were slightly increased with 40 % at concentrations of 0,01 μM and 0,1 μM. At 1 μM CTD30 raised with a 140% and CTD90 was twofold elevated. In contrast to CTD90, which was raised by a factor of 3,3 at 10 μM, CTD30 fall to a raise of 30%.

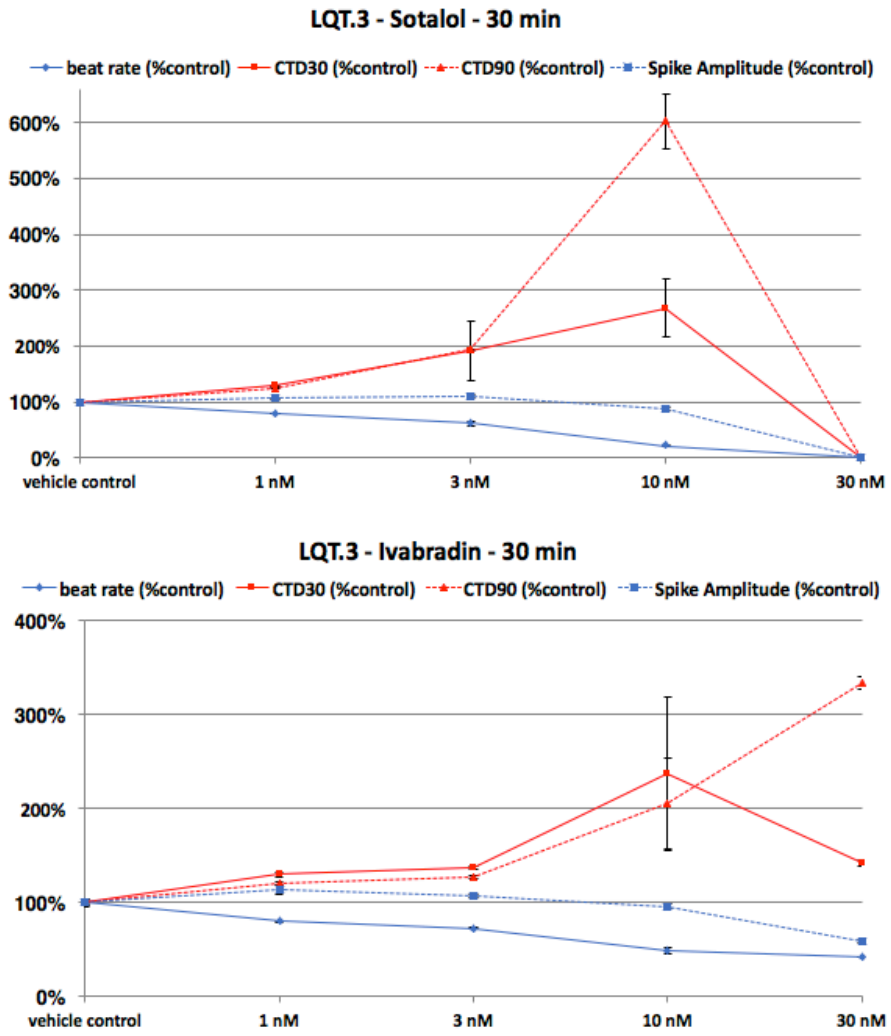

Figure 26 Calcium cycling of LQT.3 CMs showing beat rate, CTD30 and 90 and spike amplitude

3.7.4. Isoprenaline effects in LQT.3 cardiomyocytes

Isoprenaline was used as positive control. An increase in beat rate as well as a reduction in CTD30, 50 and 90 over time (figure 27) was measured.

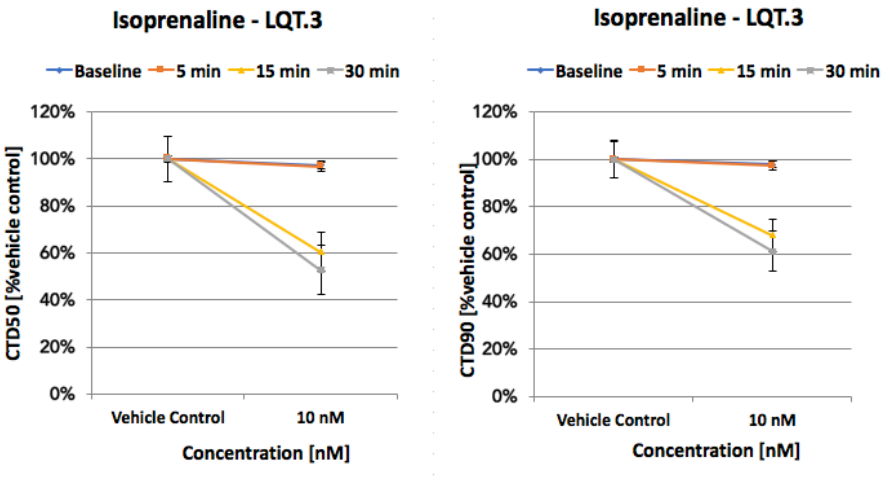

Figure 27 Calcium cycling of LQT.3 CMs after treatment with isoprenaline 10 nM. CTD 50 and 90 is displayed at baseline, after 5, 15 and 30 minutes of incubation.

3.8. Contraction force analysis of LQT.3 cardiomyocytes

3.8.1. Isoprenaline effects in LQT.3 cardiomyocytes

The positive inotrope and chronotrope catecholamine isoprenaline revealed an expected behavior. Administration of small doses starting at 10 nM raised the force amplitude by 75 % and up to 82,3 % and 82,9 % at 50 and respectively 100 nM isoprenaline. A maximum of inotropy was seen 60 minutes after incubation with 100 nM isoprenaline. Frequency was raised by 42,21 % at the starting concentration of 10 nM but afterwards diminished linear to 32,20 %. Contraction duration was dose-dependent shortened whereas relaxation duration also was shortened but at a steady interval of 16 - 28 %. Contraction and relaxation slope were both raised with a factor 2 (figure 28).

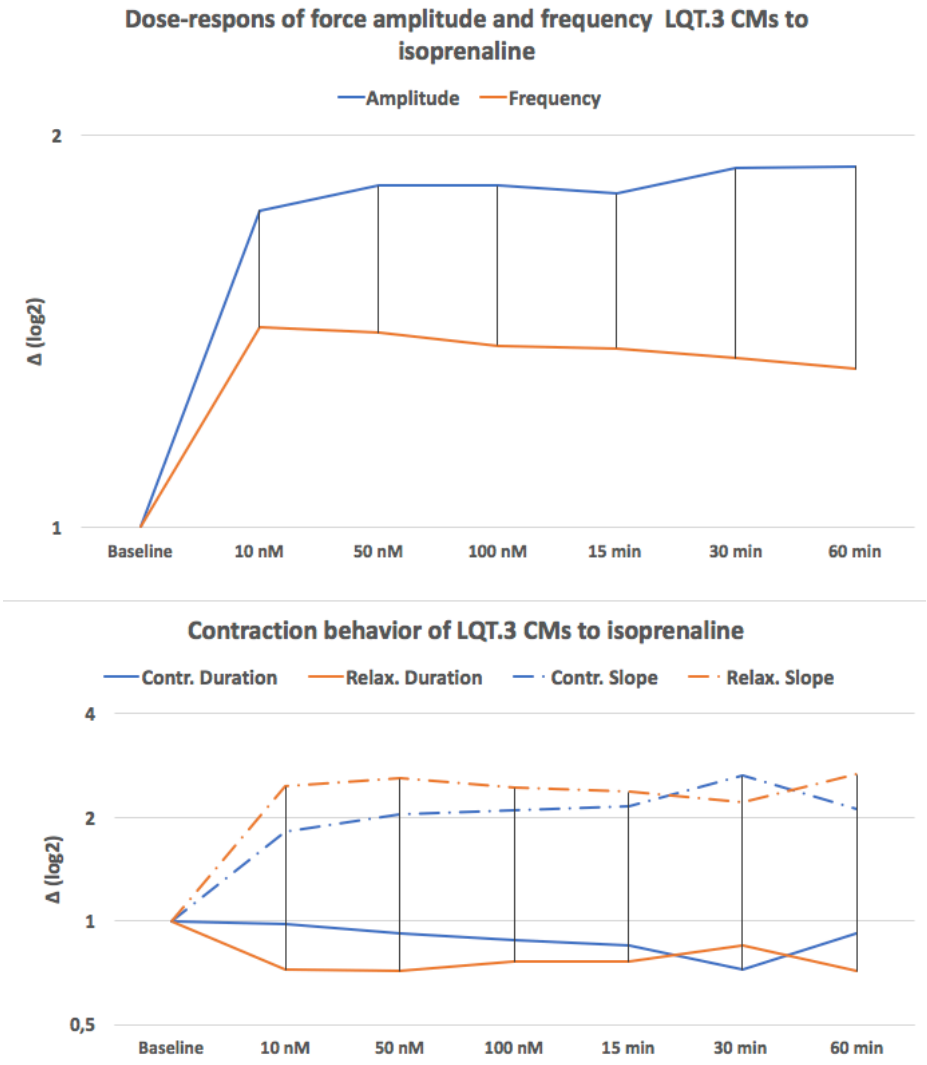

Figure 28 Effect of isoprenaline to beating behavior and contraction force of LQT.3 CMs

3.8.2. Dofetilide effects in LQT.3 cardiomyocytes

Dofetilide revealed a linear decrease in frequency. Simultaneously the force amplitude was strongly decreased with more than 50%. Isoprenaline had a positive chronotrope effect on LQT.3 CMs but did not show a positive inotrope effect and could not rescue the force amplitude. This implicates that the hERG block has a direct impact on cellular calcium homeostasis and that ß-adrenergic signaling cannot

raise contractility and thereby the cellular force. The impact on cellular calcium homeostasis is already analyzed in 3.7 (figure 29).

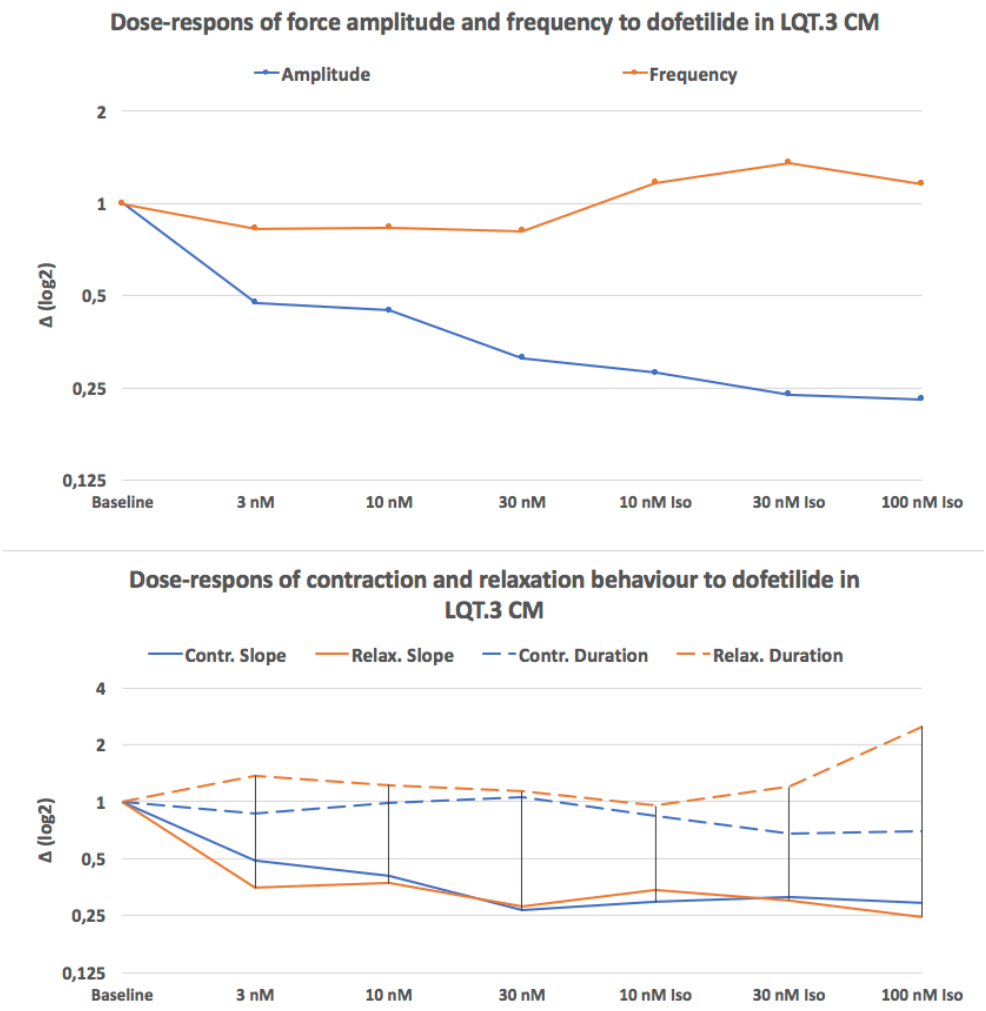

Figure 29 Change in beating behavior of LQT. CMs after dofetilide treatment

3.8.3. Verapamil effects in LQT.3 cardiomyocytes

Verapamil is a voltage-dependent Ca^{2+} channel antagonist, which leads to a decreased contractility of CMs by reducing intracellular calcium. In this contractile force assay, verapamil caused a decrease of force amplitude at 3 nM with 60 % and a beating arrest at higher concentrations. A decrease in frequency was also noted accompanied with a prolonged relaxation duration and increased contraction. LQT.3 CMs could be rescued using isoprenaline. CMs did not show an increase in amplitude above the baseline values but with a more than 50 % decreased amplitude compared to baseline measurements. Frequency recovered directly but did not exceed the baseline frequency (figure 30).

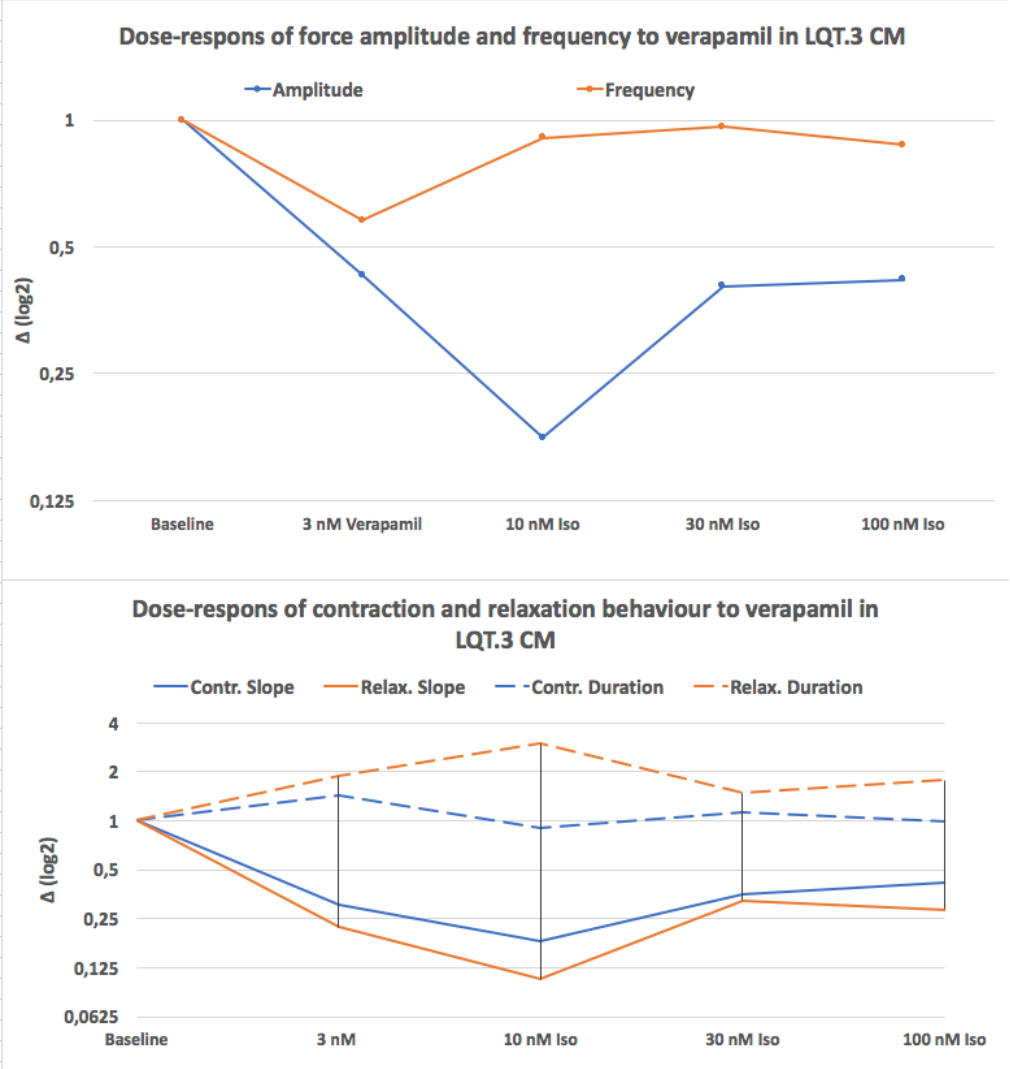

Figure 30 Verapamil induced reduction of contraction force amplitude and effect on beating behavior.

3.8.4. Mexiletine effects in LQT.3 cardiomyocytes

Mexiletine showed aspects of a light positive inotrope effect at 1 - 10 μM (increase of amplitude with 11 % respectively 5 %) and a negative inotrope effect at 30 μM (decrease of amplitude with 18 %). Frequency was diminished at all concentrations (decrease of 8 % to 23 %). The negative inotropy at 30 μM could be overcome with the positive inotrope response of 50 nM isoprenaline (26 % above baseline value). The relaxation duration was prolonged and the contraction slope is increased at 1 and 3 μM Mexiletine. Mexiletine showed an increased relaxation duration with a decreased relaxation slope which could also be overcome with 50 nM isoprenaline. At 1 μM an increased contraction slope with a diminishing of the contraction slope at higher concentration and reduced contraction slope at 30 μM (figure 31) was detected.

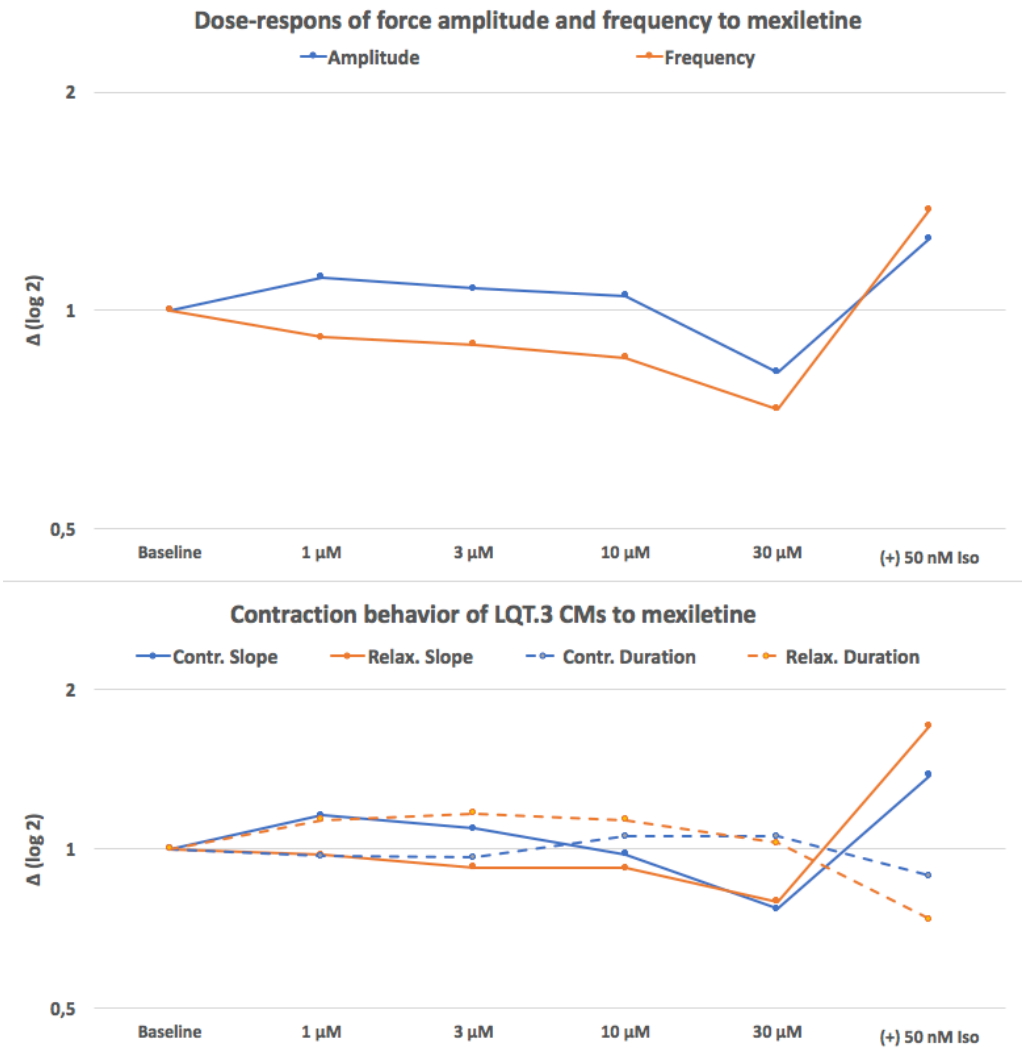

Figure 31 Force amplitude and contraction behavior for LQT.3 CMs after incubation with mexiletine.

3.8.5. Ranolazine effects in LQT.3 cardiomyocytes

Ranolazine presented with a positive inotrope effect at 3 μM (increase of amplitude with 13 %) and a negative inotrope effect starting at 10 μM (decrease of amplitude with 5 % and 25 % at 30 μM). Frequency reacted to Ranolazine with a dose-dependent reduction. Both amplitude and frequency could be rescued with 50 nM isoprenaline. Relaxation behavior was marginally influenced until a concentration of 30 μM ranolazine at which relaxation duration and contraction slope were strongly increased and contraction duration and relaxation slope decreased. This effect was also reversible with 50 nM isoprenaline. Following graphic reconstruction of beating behavior there was no decrease in frequency detected, but arrhythmic behavior could be observed at 30 μM ranolazine showing EADs and ectopic beats (figure 32).

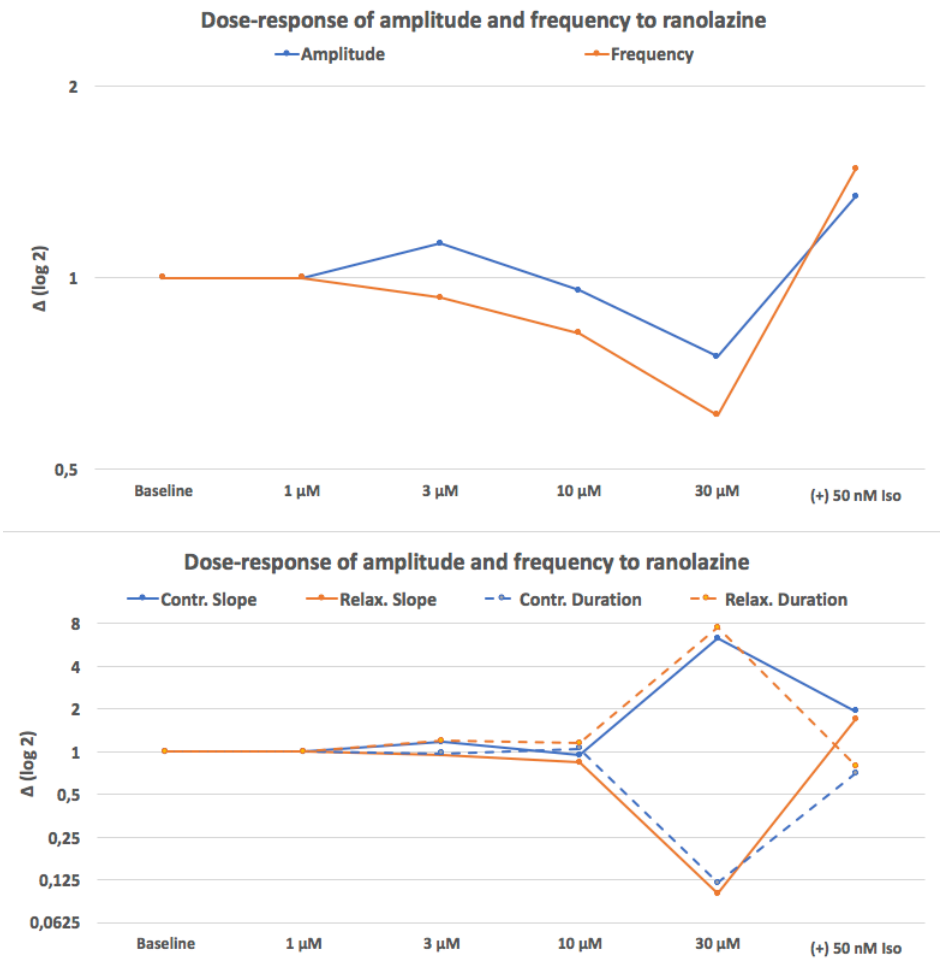

Figure 32 Contraction and relaxation behavior upon ranolazine challenge

3.8.6. Moxifloxacin effects in LQT.3 cardiomyocytes

Moxifloxacin reduced contractile force significantly with 23 % starting from the lowest dose of 3 μM (figure 33). Force amplitude was further reduced with higher moxifloxacin concentrations and could not be rescued with serial isoprenaline applications. Amplitude was also reduced significantly with 20%. Isoprenaline could also not rescue the frequency. Contraction and relaxation duration were relatively stable whereas contraction and relaxation slope were reduced over time and upping concentrations of moxifloxacin.

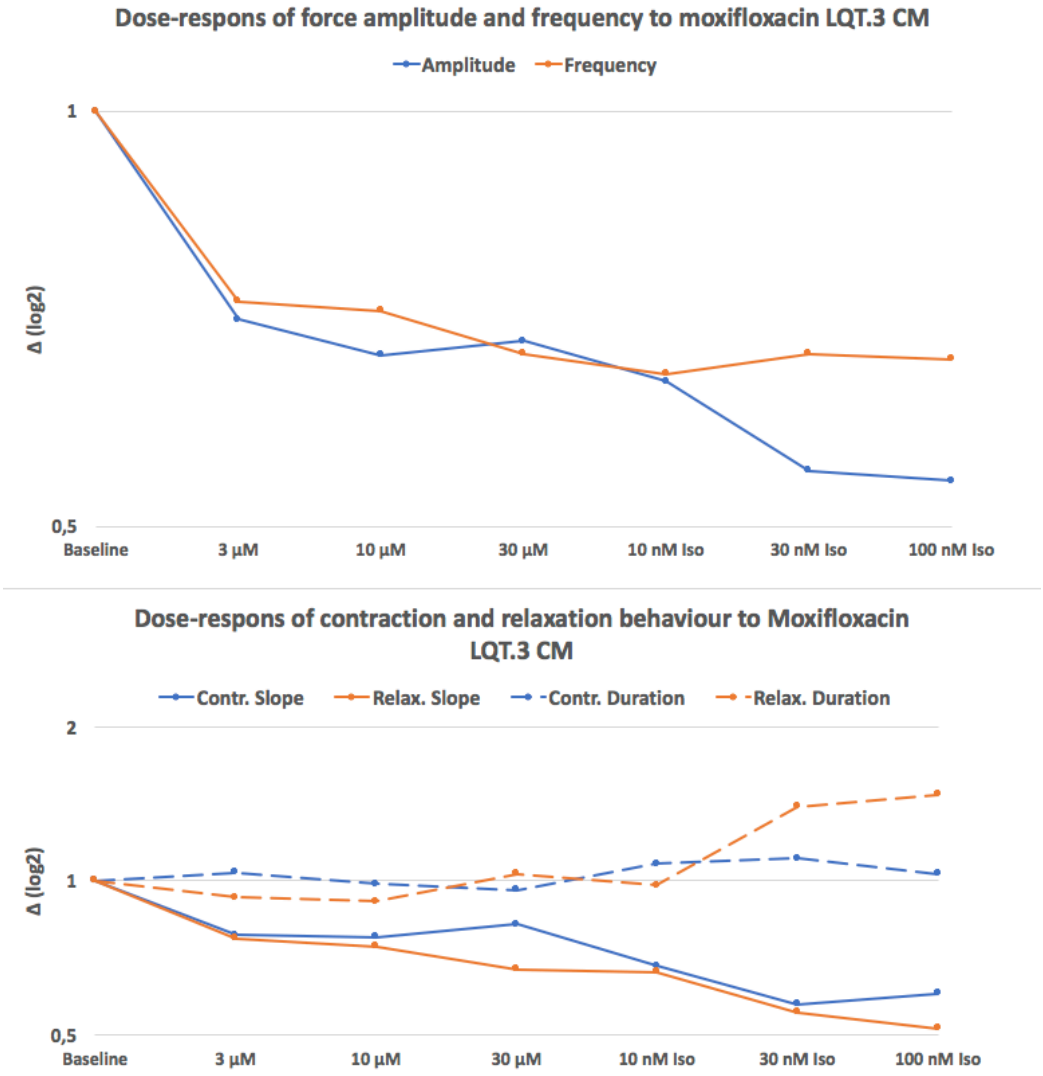

Figure 33 Contraction and relaxation behavior upon moxifloxacin challenge and serial rescue trials of contractile force in LQT.3 CM.

3.9. Optogenetic pacing of LQT.3 and CorV.4U CM

CorV.4U CMs were successfully transfected with the ChR2 mRNA. After 24 hours of recovery after transfection they showed a stable beating behavior and could be optically paced using the optical stimulation unit on MEA systems. Frequency up to 2 Hz, a light impulse of 4 ms and a conduction current of 5 mA were tested. LQT.3 could yet not successfully transfected with the ChR2 mRNA due to cytotoxicity of the compounds used. The protocol will be adapted to the needs of the LQT.3 CM. However, optogenetic pacing is preferred in future as it does not show electrical artifacts. Tyrode's solution seems to be problem solving option.

4. Discussion

In this study patient specific hiPSC were used to differentiate these cells, using small molecules, into stable beating CMs expressing the LQTS type 3 phenotype. CMs were analyzed by immunofluorescence and electrophysiological studies as MEA, impedance measurements, calcium transients as well as force measurements and patch clamp, **with the attempt to qualify the model for additional more sensitive arrhythmic studies**.

4.1. Cardiac differentiation

Cardiac differentiation with small molecules using an adherent differentiation approach is more effective than the differentiation with embryoid body formation or End2-Co-Culture [34,37]. In cardiac embryology, it is known that there are several signaling molecules that drive pluripotent cells in the beginning of gastrulation into CMs. Retinoic acid (RA), activin A and bone morphogenic protein 4 (BMP4) together with inhibition of WNT-signaling, genetic activation orchestrates a successful cardiac differentiation in vivo by inducing a mesodermal differentiation pathway [40,41,42,43]. Burridge et al. described six major pathways for the differentiation: FGF, activin-nodal, BMP, WNT and TGF-ß together with p38 MAPK being not that important as the first four pathways [35,36]. They found out that by the third to fourth day of differentiation all these differentiation-pathways were not required anymore implicating the crucial role of inhibition or induction of them in the first days of differentiation [35,36,41,42]. Taking these pathways into account, a successful differentiation of LQT.3 hiPSC into spontaneously beating CMs can be achieved by adherent differentiation and the well timed administration of small molecules [10,35,36,41]. CHIR99021, a GSK3B-inhibitor, activates WNT-signaling on the first day and hereby induces cardiac differentiation [39]. On day 2 WNT-signaling inhibitors, XAV939, together with RA and WNT-c59, were used for further cardiac differentiation by inhibiting the feedback loop of FGF-, BMP- as well as the activin- and WNT signaling pathway [36]. The results show the crucial need to pass through a directed WNT-pathway as described. Furthermore, the results prove the findings of Burridge et al. to first activate WNT-signaling and then inhibit WNT-signaling in the first three to four days of differentiation. Moreover, the majority of in-vitro purified cardiac differentiation is ensured by small molecules as proteins from the TNF family that directly interact with central elements of the WNT cycle. In general, the WNT pathway is the most prominent pathway in the differentiation of almost all end-differentiation for the in-vitro generation of specific tissue from meso-neuroectoderm and endodermal fate [43]. Spatiotemporal and concentration specific modification of the WNT cycle determines the respective differentiation fate [40,42,43]. Another approach to direct atrial or ventricular phenotype would be to influence the BMP-activin/smad pathway. Low BMP-4 and high activin A favors atrial CMs whereas high BMP-4 and low activin A induces a ventricular differentiation marking the BMP-4 pathway as an important pathway for myocardial development [42]. RA in this place supports the atrial-predominant differentiation [44]. With the successful differentiation of hiPSC derived LQT.3 CMs the crucial role of WNT pathway modulation was recapitulated in time and its concentration dependent significance. LQT.3 CMs were nearly equally differentiated as CorV.4U with differences in concentrations of small molecules due to an

optimized differentiation rate. This implicates that CorV.4U and LQT.3 CMs have a similar epigenetic pattern and are suitable for a direct comparison in electrophysiological studies.

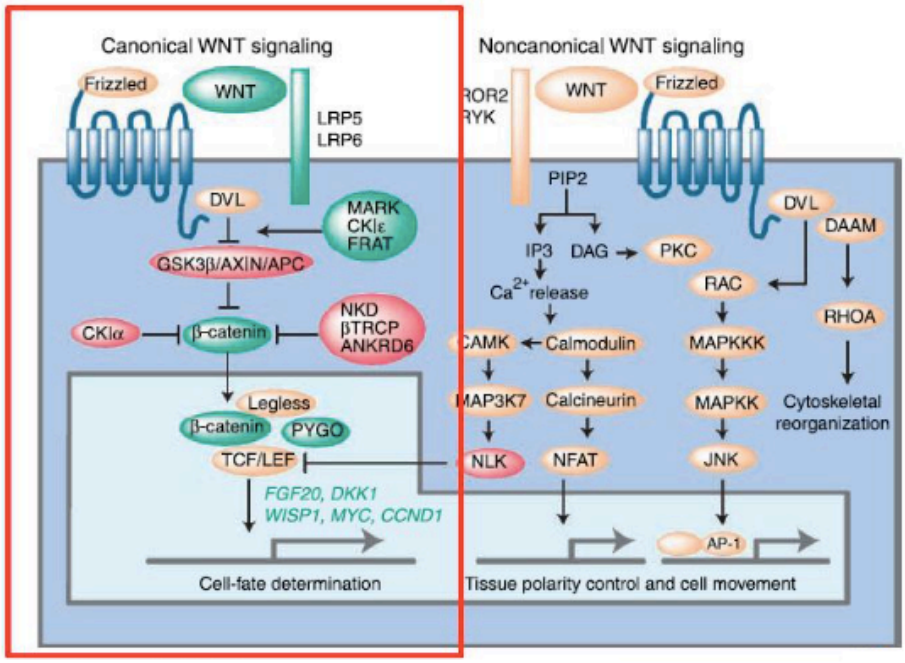

Figure 34 The WNT signaling pathway is one of the most influenced pathways in differentiation hiPSC into CMs in in-vitro studies (adopted from Katoh et al. [48]).

4.2. Phenotype description of LQT.3 cardiomyocytes

The results show that patient specific hiPSC expressing the disease genotype of the LQTS type 3 can be successfully differentiated in spontaneously beating cardiac tissue using small molecules combined with a cardiac specific expressed resistance gene for the purification of CMs. Using hiPSC eliminates the ethical concerns associated with hESC generation and the problem of inter-species extrapolation if murine stem cells are used.

Immunostaining proofed end-differentiated cell populations of CMs with a ventricular-like LQT.3 phenotype. The major intracellular proteins, myosin (MLC-2V), alpha-actinin and troponin showed high expression rates. Compared to healthy CMs (CorV.4U CMs) the phenotype was slightly different regarding Connexin40, which was negative in the LQT.3 CMs and positive in CorV.4U CMs. The other cardiac specific proteins where equally distributed and expressed. The genetic analysis of the hiPSC was conducted at Coriell and revealed a de-novo mutation in the SCN5A gene (1218C>A, N406K) by sequencing. Further electrophysiological studies confirmed the LQT.3 phenotype.

Electrophysiological analysis using MEA technique revealed a different electrophysiological phenotype of LQT.3 CMs as compared to CorV.4U. LQT.3 CMs presented with prolonged FPD of 603,79 (± 43,39) ms resembling the phenotype of a prolonged QT-interval in LQTS type 3 patients. This was proven by patch-clamp analysis with an AP > 1000 ms. In CorV.4U a FPD of 278,30 (±70,91) ms was measured using the MEA technique. Baseline ($p < 0,001$) and frequency corrected FPD, using the Bazett (FPDcB) correction formula ($p < 0,05$) and the Frederricia (FPDcF) correction formula ($p < 0,001$), were significantly increased in LQT.3 CMs when compared with CorA.4U CMs. FPDcB was significantly

increased in LQT.3 CMs compared to CorV.4U ($p < 0,05$). Furthermore, this discrepancy of FPD and AP shows the need of a physiologically relevant environment for in-vitro studies. Base-impedance measurements with an AP-duration (APD) of 550 ms (± 65 ms) proved FPD measured with MEA analysis. Cardiac force is a parameter that is not incorporated in drug safety testings in pre-clinicial in-vitro studies. The positive inotrope and chronotrope effect of isoprenaline demonstrates that cellular force measurements using the Cor.4CE® technique can be performed on LQT.3 CMs. Various other cardiac and non-cardiac drugs were tested regarding the influence of contraction force in LQT.3 CM. This establishes the possibility to detect a negative inotrope effect as an ADR during pre-clinical testings. The Fluo4 calcium sensor can be used in hiPSC derived LQT.3 CMs to study calcium transients. Calcium as a physiologically highly relevant ion in cellular homeostasis as well as a potent inductor of EADs and DADs is thought to be an important field of investigation when analyzing the effect of a certain drug. However, it remains difficult to measure arrhythmic beating behavior within this technique but the potency to induce these. Transfection of mRNA coding for an intracellular calcium sensor using the Express.4U calcium sensor would minimize alterations of the cellular environment (Tyrode's solution needed for Fluo4) and should be investigated in future experiments.

4.3. Comparison of LQT.3 and CorV.4U cardiomyocytes

The direct comparison of LQT.3 CMs and CorV.4U CMs by MEA analysis revealed a major difference in FPD prolongation as well as in the frequency corrected format by Bazetts' method. Ranolazine showed a significant increase of the FPD of LQT.3 CM. This effect can be explained by the hERG-blocking effect of ranolazine. Ranolazine is thought to reduce intracellular calcium due to sodium-dependent calcium channels on the membrane surface. Ranolazine did not shorten calcium transients in LQT.3 CMs but instead prolonging CTD90 with more than 300 % leading to the conclusion that there is no desirable effect of ranolazine to LQT.3 CM. Moreover, Hartley et al. described the phenomenon, that ranolazine did also lengthen AP and QT-interval in clinical practice by 2-6 ms [14]. This implicates that the hERG blocking effect is more sensitively detected in the LQT.3 CM. Similar to ranolazine, LQT.3 CMs showed a prolonged FPD and relative stable beat rate when treated with mexiletine. This class 1c AAR drug is a sodium channel inhibitor which is thought to shorten the FPD. On the contrary, CorV.4U did not show a prolongation of FPD after the treatment with mexiletine. Several mutations in LQTS lead to a resistance against several class 1 AAR drug-effects in the treatment of inherited heart rhythm disorders described by Huang et al. [45]. FPD measured in CorV.4U treated with moxifloxacin, a fluoroquinolone antibiotic widely used in clinical practice, were slightly elevated over time and escalating concentrations with a significantly decreased beating frequency. LQT.3 CMs in contrast showed a significantly increased FPD starting at the lowest concentration of 3 μM leading to a higher risk in the formation of EADs and arrhythmias. FPD was raised by more than 100 % at the highest concentration tested although frequency was stable over time. Calcium transients were not prolonged confirming the well known hERG blocking effect of moxifloxacin. Challenges with the hERG blocker dofetilide revealed similar effects in LQT.3 CMs and CorV.4U. FPD was nearly doubled at 10 nM and even tripled at 30 nM in LQT.3 CMs where in contrast CorV.4U showed an increase in FPD of less than 50%. As shown in figure 18, LQT.3 CMs also showed a tachyarrhythmia when treated with the highest concentration of dofetilide.

Sotalol increased FPD in both LQT.3 and CorV.4U CMs resulting in a beating arrest after 30 minutes under the highest concentration in CorV.4U CM. FPD again was more elevated in LQT.3 CMs than CorV.4U CM. The beating arrest in CorV.4U CMs and the progressive prolongation of FPD in LQT.3 CMs demonstrates the mixed properties of sotalol, being a class 2 AAR (ß-blocker) and class 3 AAR (hERG-blocker) which in this case predominantly prolongs the FPD. LQT.3 CMs are much more sensitive in analyzing hERG-channel blocks than CorV.4U CM. Ivabradine is a nodal-specific I_f-channel inhibitor resulting in a light progressive increase in FPD of 33 % with a nearly linear decrease in frequency in CorV.4U. In contrast LQT.3 CMs revealed a greater effect in FPD prolongation leading to the conclusion of more I-expressing pacemaker-like cells in the LQT.3 CMs population. FPD could not be analyzed over all concentrations due to not-detectable T-wave like signals. CMs did not show beating arrest under ivabradine treatment, but both CM populations showed a decrease in frequency. Isoproterenol was used as a positive control to test the ß-adrenergic response of in-vitro differentiated CM. Both cell lines showed an increase in frequency and slight decrease in FPD. On top, the positive inotrope effect of isoproterenol could be proven using the Cor.4CE technique measuring cell forces. Definitive FPD prolongation was tested within the negative control with E-4031, a known hERG-inhibitor. In CorV.4U FPD was increased over time and CMs developed a beating arrest at 10nM with a reduced frequency. On the other hand, LQT.3 CMs showed a stable beat rate with significantly increased FPD. This effect could be explained by a lack of E-4031 sensitive hERG-channels in the pacemaker cell population leading to a prolonged FPD together with a stable beat rate. At low frequencies and prolonged and increased FPD, beat rate can stay stable due to relative long RR-intervals.

These effects demonstrate the higher sensitivity in measuring FPD prolongation using the LQT.3 CMs model as compared to other CM models.

Taken together this study clearly demonstrates that hiPSC derived CM expressing the disease genotype- and phenotype of the LQTS type 3 offer an important advantage to study the pathophysiology of this disease. Additionally, there is no future need to harvest cardiac biopsies from affected patients with inherited rhythm disorders. By using the patient-specific LQT.3 CMs it is now feasible to test ADR that are potentially harmful for patients affected with the LQTS. This could strengthen and upgrade data bases such as incrediblemeds.org which collect data on QT prolonging drugs and potential life threatening medications if administered to patients affected with the LQTS.

One major problem in toxicological studies is the differentiation between the effects caused by a drug on different tissue or a specific cell populations. Using a cytotoxin for the purification of CMs by choosing a cardiac specific promotor for the toxin-resistance gene that was transfected into hiPSC enables the analysis of a homogenous cell population without potential disturbances created by not fully differentiated cells or differentiated cells other than CMs. Further, de-differentiated CMs can also be eliminated by re-treating the cell population with the toxic selection agent in the phase of maturation for example. Regarding the literature, maturation of CMs is essential to induce a ventricular-like phenotype in-vitro [36]. CMs show an atrial-like phenotype in the first 14-21 days after differentiation and are described as immature CMs. Approximately 6-8 weeks after differentiation CMs present with a ventricular-like phenotype. These phenotype patterns are not homogeneous over time, implicating that there will be ventricular-like CMs and nodal-like pacemaker cells present in the

beginning as well as the presence of atrial-like CMs after several weeks of differentiation [35,36]. Significant effects on LQT.3 CMs treated with ivabradine in experiments using MEA, calcium transients and force measurements, implicates the presence of I_f current ('funny current') nodal-like CMs. Ivabradine inhibits the I_f current ('funny current'), which is mainly expressed in nodal pacemaker cells. Thus, the culture is not a pure ventricular-like CM population and there are several nodal pacemaker cells present in the culture. In contrast to this, some CMs could have acquired pacemaker characteristics, leading to several ventricle-specific pacemaker CMs which orchestrate the frequency of the CM population. This theory can be confirmed with the analysis of a heat map recorded in MEA experiments. There is always one, central area where the stimulus of one coordinated CM-cluster contraction is generated.

4.4. SCN5A polymorphism and associated clinical presentation

Mutations in the SCNA5A-gene encoding the alpha-1 subunit of the $Na_V1.5$ voltage gated sodium channel, specifically expressed in cardiac tissue, are responsible for the Long QT syndrome type 3 (LQT. 3), Brugada syndrome, atrial fibrillation and dilated cardiomyopathy. This channel is responsible for the fast initiation of depolarization and action potential propagation. It consists of a single-pore forming alpha-subunit of 33 - 36 kDa forming 4 homologous transmembrane domains. Each domain itself consists of six assumed transmembrane segments. Extracellular linker regions between segment five and six of each domain join together and form channel pore (P-loop) which controls selectivity and permeability of ions. Segment 4 is responsible for fast activation of the sodium channel through its action as a voltage sensor generated by multiple positive charged amino acids such as lysine or arginine which change constitution during membrane depolarization. Responsible for fast inactivation are IFM-motifs in the extracellular region between domain III and IV and the intracellular linker of segment 4 and 5 in domain III and IV as well as in the P-loop. These IFM motifs consist of a special amino-acid triplet Ile-Phe-Met [47]. Moreover the alpha-subunit can be accompanied by several ß-subunits which have a regulatory impact. In cardiac tissue the $Na_V1.5$ sodium channel is non-covalently associated with ß1- and ß3-subunits. The expression of these subunits is associated with channel kinetics and activation processes but is yet not associated with any pathophysiology of the LQT syndrome or other channnelopathies.

The localization of SCN5A mutation is important for the phenotype of the disease. If mutations are localized in ion specificity determining regions, channel currents may be influenced giving specific phenotypes. Mutations in unspecific regions may result in asymptomatic syndromes with no or moderate prolongation of the QT interval. Not only the localization itself is essential for the clinical presentation but also the efficacy of anti-arrhythmic drugs used for this disease seems to be mutation-specific. Hereby, not all patients with the LQTS type 3 can be treated with the same medication, because some mutations lead to an inefficacy for several drugs. This implicates that mutations need to be re-evaluated regarding the extent of disease phenotype, reaction to treatment medication (different effects in different hiPSC models) as well as the risk for potential life threatening arrhythmias. Recent studies showed for example a heterogenous effect of Mexiletine sensitivity in different SCN5A mutation and recommended a mutation specific patient treatment approach [1].

4.5. Future aspects

In the present study, LQT.3 CMs were compared with CorV.4U. Although being equally differentiated and thereby epigenetic analogical, these cell lines have different donors and thereby a different imprinting. A solution to this problem could be the usage of only one well defined cell line. Healthy CMs (CorV.4U for example) can be transfected with a mutated mRNA of the SCN5A gene using the Express.4U technique. Hereby, healthy CMs can be measured before the transfection to generate baseline values. In a second step, these healthy CMs are transfected to induce a disease phenotype that can directly be compared within the same CM. This would give scientists the possibility to make more advanced experiments in pharmacological studies. Furthermore, there would be no need to establish disease models anymore. Many disease models can be induced in-vitro by using one standardized cell line which is transfected with mRNA of a gene that causes a certain disease. The advantages in using mRNA transfection by the Express.4U are minor cell manipulation, low workload, very high efficiency and low toxicity. On the other hand, production of stable capped mRNA is relatively cost extensive. The amount of work and costs associated with producing and characterizing a disease model in-vitro must not be underestimated. Furthermore, the transfection protocol seems to be adjusted to CM models.

This study describes the pharmacological experiments that can be conducted with such a cell model and the possibility to identify substances reducing the FPD and thereby reducing the risk of TdP. Future experiments could be extended to cure the LQTS phenotype by CRISPR/Cas modification of the mutated SCN5A gene. Hereby, the mutated gene is cut out of the genome and replaced by a wild-type non-mutated gene sequence leading to the expression of a normal functioning NaV1.5. Healthy CM (CorV.4U) can also be manipulated by CRISPR/Cas modulated insertion of mutated SNC5A genes in a mono- or bi-allelic approach. Another way to possibly address the disease phenotype would be to transfect affected CMs with an anti-sense mRNA blocking the mRNA expressed by the mutated SCN5A gene and a simultaneous transfection with non-mutated mRNA of the respective channel which would replace the LQTS phenotype by a healthy phenotype. In this approach, curing would be temporary whereas the genetic modification with CRISPR/Cas would be a definitive solution because the germline is changed. However, this remains difficult due to ethical concerns and regulation of modified cells in-vivo as well as the challenging aspects in the combination of germline modification and simultaneous use of Express.4U.

5. Acknowledgments

I especially would like to thank Prof. Dr. Brugada for his knowledge and passionate support during the writing of the thesis. Prof. Dr. Brugada is an intellectual mentor who tirelessly offered counsel and advice. For his innumerable gifts and time I am grateful. I also would like to acknowledge Axiogenesis for the laboratories and materials that were used in this study, Ralf Kettenhofen and Dietmar Hess for the input during the electrophysiological characterization of the LQT.3 CM. Further, I would like to thank Melanie Fahrendorf, Alina Prot and Noushin and Andreas Ehlich for their support in the laboratory work. Last but not least I wish to thank my father for his teaching in laboratory skills and exemplary traits of character.

6. Conflicts of interest

The author declares a conflict of interest in the matter that he has been former shareholder of stocks linked to the origin of the hiPSC at Axiogenesis AG.

7. Bibliography

1. Schwartz, PJ et al.. Diagnostic criteria for the long QT syndrome. an update. *Circulation*, 1993, 88(2), pp.782–784. Available at: http://circ.ahajournals.org/cgi/doi/10.1161/01.CIR.88.2.782
2. Mizusawa Y, Horie M. & Wilde A. Genetic and clinical advances in congenital long QT syndrome. *Circulation Journal*, 2014, 78(12), pp.2827–2833. Available at: http://jlc.jst.go.jp/DN/JST.JSTAGE/circj/CJ-14-0905?lang=en&from=CrossRef&type=abstract
3. MD et al 2015??
4. Schwartz, PJ, Crotti, L & Insolia, R. Long-QT syndrome: From genetics to management. *Circulation: Arrhythmia and Electrophysiology*, 2012, 5(4), pp.868–877. Available at: http://circep.ahajournals.org/cgi/doi/10.1161/CIRCEP.111.962019
5. Mizusawa Y & Wilde A. QT prolongation and mortality in hospital settings: Identifying patients at high risk. *Mayo Clinic Proceedings*, 2013, 88(4), pp.309–311. Available at: http://dx.doi.org/10.1016/j.mayocp.2013.02.004
6. Alders, M & Christiaans, I. Long QT Syndrome - NCBI Bookshelf. In *Gene Review*. 2003, pp. 1–26. Available at: https://www.ncbi.nlm.nih.gov/books/NBK1129/?report=printable
7. Ackermann & Tester et al. Genetics of Long QT Syndrome. Methodist Debakey Cardiovasc J. 2014 Jan-Mar; 10(1): 29–33. 2014, pp.1–5. Available at: https://www.ncbi.nlm.nih.gov/pmc/articles/PMC4051331
8. Schwartz, PJ et al. The Jervell- and Lange-Nielsen syndrome: Natural history, molecular basis, and clinical outcome. *Circulation*, 2006, pp.783–790. Available at: http://circ.ahajournals.org/cgi/doi/10.1161/CIRCULATIONAHA.105.592899
9. Amin, AS, Pinto, YM & Wilde, AAM. Long QT syndrome: Beyond the causal mutation. *The Journal of Physiology*, 2013, 591(17), pp.4125–4139. Available at: http://doi.wiley.com/10.1113/jphysiol.2013.254920
10. Terrenoire, C. et al.. Induced pluripotent stem cells used to reveal drug actions in a long QT syndrome family with complex genetics. *The Journal of General Physiology*, 2012, 141(1), pp.61–72. Available at: http://www.jgp.org/lookup/doi/10.1085/jgp.201210899
11. Schwartz, P.J. et al. Prevalence of the congenital long-qT syndrome. *Circulation*, 2009, 120(18), pp.1761–1767. Available at: http://circ.ahajournals.org/cgi/doi/10.1161/CIRCULATIONAHA.109.863209
12. Qureshi, S.F. et al. Novel mutations of kCNQ1 in long QT syndrome. *Indian Heart Journal*, 2013, 65(5), pp.552–560. Available at: http://dx.doi.org/10.1016/j.ihj.2013.08.025
13. Brugada, P, Brugada, J & Roy, D. Brugada syndrome 1992-2012: 20 years of scientific excitement, and more. *European Heart Journal*, 2013, 34(47), pp.3610–3615. Available at: https://academic.oup.com/eurheartj/article-lookup/doi/10.1093/eurheartj/eht113
14. Rayner-Hartley, E. & Sedlak, T.. Ranolazine: A contemporary review. *Journal of the American Heart Association*, 2016, 5(3). Available at: http://jaha.ahajournals.org/lookup/doi/10.1161/JAHA.116.003196
15. Amin AS, Asghari-Roodsari, A. & Tan, HL. Cardiac sodium channelopathies. *Pflügers Archiv - European Journal of Physiology*,2009, 460(2), pp.223–237. Available at: http://link.springer.com/10.1007/s00424-009-0761-0
16. Ikonnikov, G. & Yelle, D. Physiology of cardiac contraction and contractility. 2013. Available at: http://www.pathophys.org/physiology-of-cardiac-conduction-and-contractility/#Electrophysiology
17. Olliaro, P.L. et al. Effects on the QT interval of a gatifloxacin-containing regimen versus standard treatment of pulmonary tuberculosis. *Antimicrobial Agents and Chemotherapy*, 2017, 61(7), p.NaN–NaN. Available at: http://aac.asm.org/lookup/doi/10.1128/AAC.01834-16
18. Woosley, R.L. Combined list of drugs that prolong QT and/or cause tdP. , 2017, pp.1–2. Available at: www.incrediblemeds.org
19. Lorberbaum, T. et al. An integrative data science pipeline to identify novel drug interactions that prolong the QT interval. *Drug Safety*, 2016, 39(5), pp.433–441. Available at: http://dx.doi.org/10.1007/s40264-016-0393-1
20. Hoekstra, M. & Wilde, AAM.. Induced pluripotent stem cell derived cardiomyocytes as models for cardiac arrhythmias. 2012, Front Physiol. 2012; 3: 346

21. Rast, G. et al.. Influence of field potential duration on spontaneous beating rate of human induced pluripotent stem cell-derived cardiomyocytes: Implications for data analysis and test system selection. *Journal of Pharmacological and Toxicological Methods*, 2016, 82(C), pp.74–82. Available at: http://dx.doi.org/10.1016/j.vascn.2016.08.002
22. Sager et al. Rechanneling the cardiac proarrhythmia safety paradigm: A meeting report from the cardiac safety research consortium. *American Heart Journal*, 2014, 167(3), pp.292–300. Available at: http://dx.doi.org/10.1016/j.ahj.2013.11.004
23. Kanda et al. Points to consider for a validation study of iPS cell-derived cardiomyocytes using a multi-electrode array system. *Journal of Pharmacological and Toxicological Methods*, 2016, 81(C), pp.196–200. Available at: http://dx.doi.org/10.1016/j.vascn.2016.06.007
24. Kofron, CM & Mende, U. In vitromodels of the cardiac microenvironment to study myocyte and non-myocyte crosstalk: Bioinspired approaches beyond the polystyrene dish. *The Journal of Physiology*, 2017, 595(12), pp.3891–3905. Available at: http://doi.wiley.com/10.1113/JP273100
25. Kitaguchi et al. CSAHi study: Evaluation of multi-electrode array in combination with human iPS cell-derived cardiomyocytes to predict drug-induced QT prolongation and arrhythmia — effects of 7 reference compounds at 10 facilities. *Journal of Pharmacological and Toxicological Methods*, 2016, 78(C), pp.93–102. Available at: http://dx.doi.org/10.1016/j.vascn.2015.12.002
26. Spencer, C.I. et al. Calcium transients closely reflect prolonged action potentials in iPSC models of inherited cardiac arrhythmia. *Stem Cell Reports*, 2014, 3(2), pp.269–281. Available at: http://dx.doi.org/10.1016/j.stemcr.2014.06.003.
27. Babbe, S. Corriel Certificate of analysis. 2014, pp.1–7. Available at: https://www.coriell.org/0/Sections/Search/Sample_Detail.aspx?Ref=GM25267&PgId=166
28. Kettenhofen et al. Frequency-Dependent Multi-Well Cardiotoxicity Screening Enabled by Optogenetic Stimulation. International Journal of Molecular Sciences. 2017 Dec; 18(12): 2634
29. Hassinen, M., Haverinen, J. & Vornanen, M. Electrophysiological properties and expression of the delayed rectifier potassium (eRG) channels in the heart of thermally acclimated rainbow trout. *AJP: Regulatory, Integrative and Comparative Physiology*, 2008, 295(1), pp.R297–R308. Available at: http://ajpregu.physiology.org/cgi/doi/10.1152/ajpregu.00612.2007
30. Walker, JM. *Patch-clamp methods and protocols* 2. Edition. In: J. M. Walker, M. Martina, & S. Taverna, eds. *Patch-clamp*. School of Life Sciences University of Hertfordshire: Springer New York. pp 159-172
31. Walker, JM. *Patch-clamp methods and protocols* 2. Edition. In: J. M. Walker, M. Martina, & S. Taverna, eds. *Patch-clamp*. School of Life Sciences University of Hertfordshire: Springer New York. pp 206-212
32. Walker, JM. *Patch-clamp methods and protocols* 2. Edition. In: J. M. Walker, M. Martina, & S. Taverna, eds. *Patch-clamp*. School of Life Sciences University of Hertfordshire: Springer New York. pp 208
33. Kempf, H., Andree, B. & Zweigerdt, R. Large-scale production of human pluripotent stem cell derived cardiomyocytes. *Advanced Drug Delivery Reviews*, 2016, 96(C), pp.18–30. Available at: http://dx.doi.org/10.1016/j.addr.2015.11.016
34. Bhattacharya, S. et al. High efficiency differentiation of human pluripotent stem cells to cardiomyocytes and characterization by flow cytometry. *Journal of Visualized Experiments*, 2014, (91), pp.1–12. Available at: http://www.jove.com/video/52010/high-efficiency-differentiation-human-pluripotent-stem-cells-to
35. Burridge, P.W. et al. Production of de novo cardiomyocytes: Human pluripotent stem cell differentiation and direct reprogramming. *Cell Stem Cell*, 10(1), 2012, pp.16–28. Available at: http://linkinghub.elsevier.com/retrieve/pii/S1934590911005947
36. Burridge, P.W. et al. Chemically defined generation of human cardiomyocytes. *Nature Methods*, 2014, pp.1–10. Available at: http://dx.doi.org/10.1038/nmeth.2999
37. Talkhabi, M., Aghdami, N. & Baharvand, H. Human cardiomyocyte generation from pluripotent stem cells: A state-of-art. *Life Sciences*, 2016, 145, pp.98–113. Available at: http://linkinghub.elsevier.com/retrieve/pii/S0024320515301144.
38. El-Haou, S et al. In depth profiling of human iPSC cardiomyocytes: From electrophysiology to phenotypic assays. Available at: www.metrionbiosciences.com
39. Cao, N. et al. Ascorbic acid enhances the cardiac differentiation of induced pluripotent stem cells through promoting the proliferation of cardiac progenitor cells. *Nature Publishing Group*, 2011, 22(1), pp.219–236. Available at: http://dx.doi.org/10.1038/cr.2011.195
40. Lin, C.J. et al. Partitioning the heart: Mechanisms of cardiac septation and valve development. *Development*, 2012, 139(18), pp.3277–3299. Available at: http://dev.biologists.org/cgi/doi/10.1242/dev.063495

41. Gessert, S. & Kühl, M. The multiple phases and faces of wnt signaling during cardiac differentiation and development. *Circulation Research*, 2010, 107(2), pp.186–199. Available at: http://circres.ahajournals.org/cgi/doi/10.1161/circresaha.110.221531
42. Wittig, J. & Münsterberg, A. The early stages of heart development: Insights from chicken embryos. *Journal of Cardiovascular Development and Disease*, 2016, 3(2), pp.12–15. Available at: http://www.mdpi.com/2308-3425/3/2/12
43. Ruiz-Villalba A, Hoppler & van den Hoff. Wnt signalling in the heart fields: Variations on a common theme. Developmental Dynamics, 2016, 245(3):294-306. doi: 10.1002/dvdy.24372. Available at: https://onlinelibrary.wiley.com/doi/abs/10.1002/dvdy.24372
44. Schneider. Upstairs, downstairs: Atrial and ventricular cardiac myocytes from human pluripotent stem cells. *Stem Cell*, 2017, 21(2), pp.151–152. Available at: http://dx.doi.org/10.1016/j.stem.2017.07.006
45. Huang, H. et al. Y1767C, a novel sCN5A mutation, induces a persistent Na+ current and potentiates ranolazine inhibition of NaV1.5 channels. *AJP: Heart and Circulatory Physiology*, 300(1), 2011, pp.H288–H299. Available at: http://ajpheart.physiology.org/cgi/doi/10.1152/ajpheart.00539.2010
46. Rajamohan, D. et al. Automated electrophysiological and pharmacological evaluation of human pluripotent stem cell-derived cardiomyocytes. *Stem Cells and Development*, 2016, 25(6), pp.439–452. Available at: http://online.liebertpub.com/doi/10.1089/scd.2015.0253
47. Song, W. & Shou, W. Cardiac sodium channel nav1.5 mutations and cardiac arrhythmia. *Pediatric Cardiology*, 2012, 33(6), pp.943–949. Available at: http://link.springer.com/10.1007/s00246-012-0303-y
48. Katoh et al. WNT Signaling Pathway and Stem Cell Signaling Network. Molecular Pathways, 2007, DOI: 10.1158/1078-0432.CCR-06-2316

8. Abbreviations

Action potential (AP), Action potential duration (APD), Action potential amplitude (APA)
Adverse drug reaction (ADR)
Antibody (AB), Antibodies (ABs)
Anti-arrhythmic drug (AAR)
Beat rate regularity index (BRRI)
Beats per minute (bpm)
Bone morphogenetic protein (BMP)
Calcium (Ca, Ca^{2+})
Calcium transient duration (CTD)
Cardiomyocyte (CM), Cardiomyocytes (CMs)
Channel Rhodopsin 2 (ChR2)
Comprehensive in-vitro Proarrhtymia Assay (CiPA)
Dimethyl-sulfoxid (DMSO)
Delayed after-depolarization (DAD)
Early after-depolarization (EAD)
Electrocardiogram (ECG)
Fibroblast growth factor (FGF)
Field Potential (FP), Field Potential Duration (FPD), Frederricia corrected FPD (FPDcF), Bazett corrected FPD (FPDcB)
Heart-rate corrected QT interval (QTc)
Human induced pluripotent stem cells (hiPSC)
Internal ribosomal splicing site (IRES)
Iscove's modified Dulbecco's medium (IMDM)
Late sodium current ($I_{Na,L}$)
Long QT syndrome (LQTS)
Long QT syndrome type 3 (LQT.3)
Magnesium (Mg, Mg^{2+})
Milliseconds (ms)
Messenger ribonucleotide acid (mRNA)
Multielectrode array (MEA)
Myosin light chain (MLC)
Nanion Sensor Plate® (NSP)
Native Goat Serum (NGS)

Phosphate buffered saline (PBS), Phosphate buffered saline without calcium and/or magnesium (PBS w/o Ca/Mg)
Peak width (PW)
Retinoic acid (RA)
Resting membrane potential (RMP)
Room temperature (RT)
Sudden cardiac death (SCD)
Torsade de pointes (TdP)
Triggered activities (TA)
Wingless- and Int-genes (WNT)

9. List of figures

10. List of table

11. Supplemental data

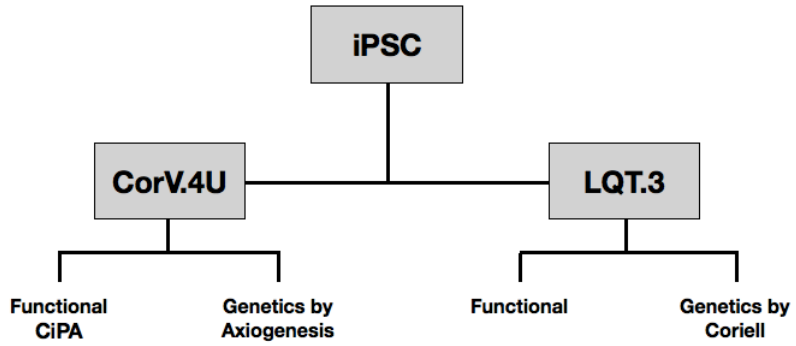

Figure 35 Basic information for the comparison of iPSC derived CM. CorV.4U and LQT.3 CMs were both differentiated from hiPSC and genetically characterized as well as functional described with electrophysiological studies in in-vitro experiments.

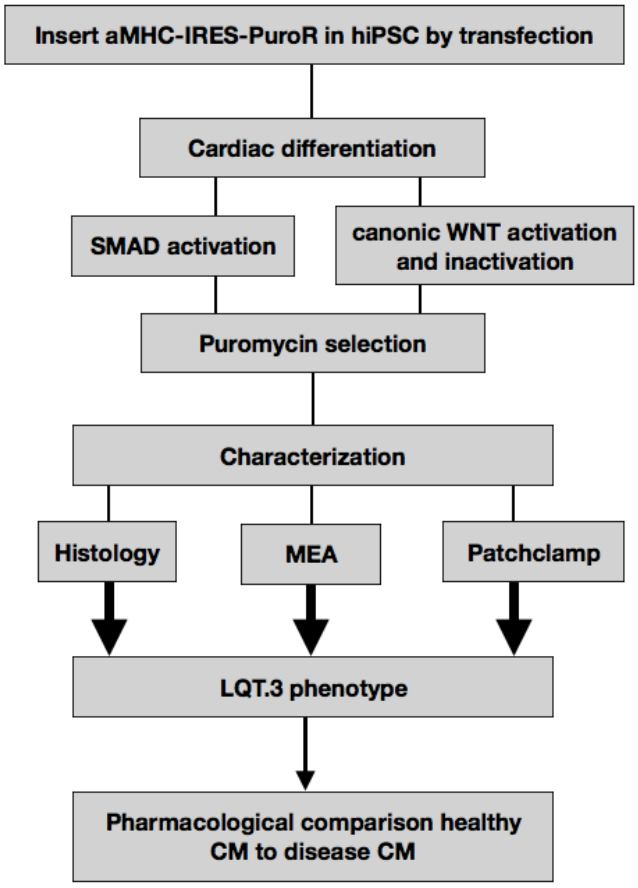

Figure 36 Flow-chart of the steps from a cardiac differentiation to pharmacological studies. HiPSC were differentiated using a cardiac specific promotor linked with an IRES site and a puromycin resistance gene; thus only cardiac cells will be resistant to puromycin. Cardiac differentiation was initiated by SMAD activation and canonic WNT activation followed by WNT inhibition. CMs were selected with puromycin and characterized by histology stainings, MEA measurements and patch clamping which revealed the hypothesized LQT.3 phenotype. Pharmacological comparisons with healthy CMs completed the analysis and characterization of this cell line.